

University of Louisville

## ThinkIR: The University of Louisville's Institutional Repository

---

Electronic Theses and Dissertations

---

12-2014

# Fabrication and characterization of antioxidant loaded liposomes.

Brian Gettler

Follow this and additional works at: <https://ir.library.louisville.edu/etd>



Part of the [Biomedical Engineering and Bioengineering Commons](#)

---

### Recommended Citation

Gettler, Brian, "Fabrication and characterization of antioxidant loaded liposomes." (2014). *Electronic Theses and Dissertations*. Paper 2277.

<https://doi.org/10.18297/etd/2277>

This Master's Thesis is brought to you for free and open access by ThinkIR: The University of Louisville's Institutional Repository. It has been accepted for inclusion in Electronic Theses and Dissertations by an authorized administrator of ThinkIR: The University of Louisville's Institutional Repository. This title appears here courtesy of the author, who has retained all other copyrights. For more information, please contact [thinkir@louisville.edu](mailto:thinkir@louisville.edu).

FABRICATION AND CHARACTERIZATION OF ANTIOXIDANT LOADED  
LIPOSOMES

By

Brian Gettler  
B.Eng., University of Louisville, 2014

A Thesis  
Submitted to the Faculty of the  
University of Louisville  
J. B. Speed School of Engineering  
As Partial Fulfillment of the Requirements  
For the Professional Degree

MASTER OF ENGINEERING

Department of Bioengineering

December 2014



FABRICATION AND CHARACTERIZATION OF ANTIOXIDANT LOADED  
LIPOSOMES

Submitted by: \_\_\_\_\_  
Brian Gettler

A Thesis Approved On

\_\_\_\_\_  
(Date)

By the Following Reading and Examination Committee:

\_\_\_\_\_  
Dr. Patricia Soucy, Thesis Director

\_\_\_\_\_  
Dr. William Ehringer

\_\_\_\_\_  
Dr. Martin O'Toole

\_\_\_\_\_  
Dr. Peter Quesada

## ACKNOWLEDGEMENTS

Special thanks to my thesis director, Dr. Patricia Soucy, and to Dr. William Ehringer for their exceptional guidance and mentorship. Thank you to Dr. Archana Akalkotkar, Dhru Patel, and Matt Kelecy for their contributions to this work. Additionally thank you to the past and present members of the Soucy lab. I would also like to acknowledge NASA for providing funds for this work and University of Louisville for my time as a student. And as always, thank you to my friends and family for supporting and generally putting up with me.

## ABSTRACT

Radiation exposure is both a major obstacle in space exploration and an occupational hazard for various careers causing DNA damage and ROS. In order to reduce the effects of radiation, the primary and most explored approach has been focused around mitigation in terms of exposure duration, exposure intensity, and shielding usage. In some situations none of these reduction strategies were viable and so the use of antioxidants is being explored as an alternate strategy for therapeutic purposes. One such antioxidant is curcumin, otherwise known as diferuloylmethane, is a component of turmeric with both antioxidant properties and anti-inflammatory properties. Another antioxidant that could be used to scavenge free radicals, n-Acetylcysteine (NAC), is both a pharmaceutical drug and a dietary supplement. Finally n-2-mercaptopropionyl glycine (N-MPG) is an antioxidant used in the treatment of kidney stones. These radioprotectants are used primarily to mitigate ROS induced by radiation but have short half-lives in physiological conditions and poor bioavailability.

Liposomes can be used to entrap materials such as NAC, N-MPG, and curcumin. Liposomes can entrap hydrophobic molecules such as curcumin within the bilayer itself or hydrophilic materials such as NAC and N-MPG within the aqueous interior of the liposome. Liposomes can be used to deliver their contents to cells via membrane fusion. Small unilamellar vesicles (SUVs) were fabricated by sonication for this purpose and SUVs were evaluated according to size, toxicity, and antioxidant capacity.

Dynamic Light Scattering (DLS) measurements showed that the limiting hydrodynamic radius of the SUVs had been reached for all conditions. Limiting

hydrodynamic radius was approximately 130nm for Soy-PC/DOTAP loading conditions and approximately 140nm for DOPC/POPA loading conditions. SEM imaging confirmed both spherical and unilamellar morphology of SUVs. Theoretical encapsulation efficiency (EE) was near 100% for curcumin loading conditions. For both NAC and N-MPG, EEs were calculated to be 0.88% and 0.90% for Soy-PC/DOTAP and DOPC/POPA loading conditions respectively. MTT assays showed no significant cytotoxicity at the concentrations of both antioxidant and lipid that were used for future evaluations. Amplex Red assay results showed that the fabrication process did not significantly reduce the antioxidant capacity of Soy-PC/DOTAP loaded with NAC or curcumin. Based on these results, it was recommended that Soy-PC/DOTAP loaded with curcumin be investigate for further use.

## TABLE OF CONTENTS

	<u>PAGE</u>
APPROVAL PAGE.....	iii
ACKNOWLEDGEMENTS.....	iv
ABSTRACT.....	v
NOMENCLATURE.....	viii
LIST OF TABLES.....	x
LIST OF FIGURES.....	xi
I.    INTRODUCTION.....	13
1.1 Background.....	13
1.2 Antioxidants.....	15
1.3 Lipid Vesicles.....	18
1.4 Objective.....	21
II.   METHODS.....	23
2.1 SUV Fabrication.....	23
2.2 DLS Size analysis.....	24
2.3 SEM Imaging.....	25
2.4 Theoretical Loading Efficiency.....	25
2.5 Cellular Uptake of Curcumin from SUVs.....	26
2.6 HDF Cell Culture.....	26
2.7 MTT Assay for Cytotoxicity.....	27
2.8 Lipid Hydroperoxidation.....	27
2.9 Antioxidant Capacity.....	28
III.  RESULTS AND DISCUSSION.....	30
3.1 SUV Fabrication.....	30
3.2 SEM Imaging for Morphology.....	33
3.3 SUV Cytotoxicity.....	37
3.4 SUV Antioxidant Capacity.....	44
3.4.1 Lipid Hydroperoxidation.....	44
3.4.2 Pre-Incubation Time for Amplex Red Assay.....	45
3.4.3 Amplex Red Assay.....	47
IV.  CONCLUSIONS, DISCUSSION, AND RECOMMENDATIONS.....	53
V.   REFERENCES.....	56
VITA.....	59



## NOMENCLATURE

ROS=Reactive Oxygen Species

LET=Linear Energy Transfer

DMTHC=Dimethyltetrahydrocurcumin

NAC=N-Acetylcysteine

N-MPG=N-2-Mercaptopropionyl Glycine

Soy-PC=Soy-Phosphatidylcholine

DOTAP=1,2-dioleoyl-3-trimethylammonium-propane

DOPC=1,2-dioleoyl-*sn*-glycero-3-phosphocholine

POPA=1-palmitoyl-2-oleoyl-*sn*-glycero-3-phosphate

SUV=Large Unilamellar Vesicle

SUV=Small Unilamellar Vesicle

HBSS=Hanks Balanced Salt Solution

DLS=Dynamic Light Scattering

SEM=Scanning Electron Microscope

HDF=Human Dermal Fibroblast

MTT=3-(4,5-Dimethylthiazol-2-yl)-2,5-Diphenyltetrazolium Bromide

HRP=Horseradish Peroxidase

B/M=Buffer Diluted Media

SD0=Soy-PC/DOTAP SUVs with 0% antioxidant (unloaded)

SDC1,SDC2,SDC10=Soy-PC/DOTAP SUVs loaded with 1%, 2%, 10% curcumin

SDN1,SDN2,SDN10=Soy-PC/DOTAP SUVs loaded with 1%, 2%, 10% NAC

SDM1,SDM2,SDM10=Soy-PC/DOTAP SUVs loaded with 1%, 2%, 10% N-MPG

DP0= DOPC/POPA SUVs with 0% antioxidant (unloaded)

DPC1,DPC2,DPC10=DOPC/POPA SUVs loaded with 1%, 2%, 10% curcumin

DPN1,DPN2,DPN10=DOPC/POPA SUVs loaded with 1%, 2%, 10% NAC

DPM1,DPM2,DPM10=DOPC/POPA SUVs loaded with 1%, 2%, 10% N-MPG

C10=Free (unloaded) Curcumin at an equivalent concentration to 10% loaded curcumin

N10= Free (unloaded) NAC at an equivalent concentration to 10% loaded NAC

M10= Free (unloaded) N-MPG at an equivalent concentration to 10% loaded N-MPG

## LIST OF TABLES

TABLE	PAGE
1. Size Analysis of Mean Diameter vs Sonication Times for Soy-PC/DOTAP SUVs...	32
2. Size Analysis of Mean Diameter vs Sonication Times for DOPC/POPA SUVs.....	33
3. Size Analysis of Mean Diameter vs Sonication Times for Extended Sonication Times.....	33
4. SUV Sizes at Production Sonication Times.....	34

## LIST OF FIGURES

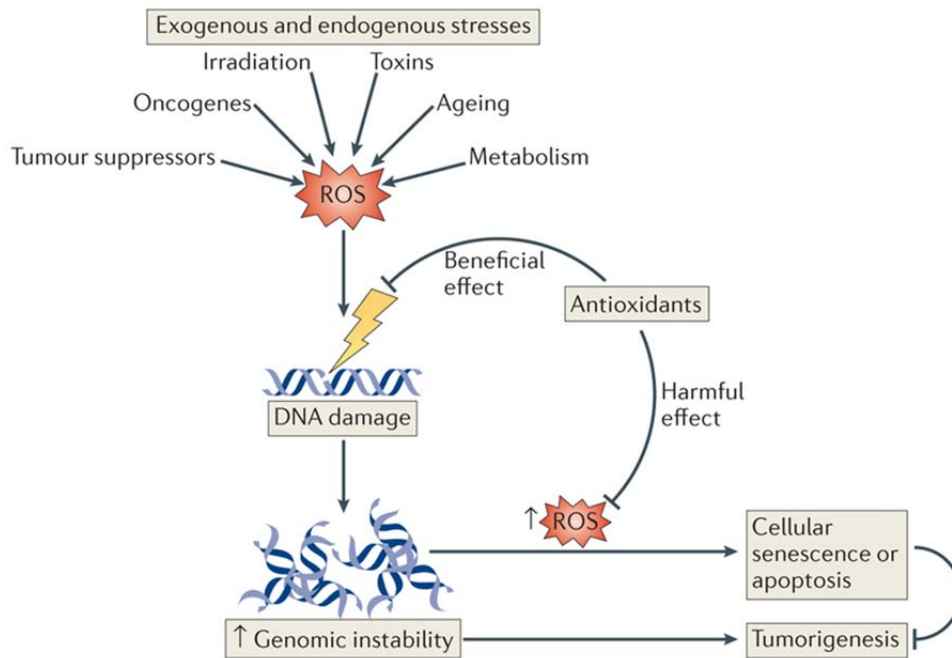
FIGURE	PAGE
1. DNA Damage through Ionized Radiation and Antioxidant Benefit .....	13
2. Curcumin Molecular Structure.....	16
3. Reaction Pathway of Curcumin with Oxidizing Radicals.....	16
4. Curcumin Degradation Products.....	17
5. NAC Molecular Structure.....	18
6. Disulfide Bridge Formation.....	18
7. N-MPG Molecular Structure.....	19
8. Curcumin Containing Lipid Vesicle.....	20
9. Soy-PC Primary Species Molecular Structure.....	21
10. DOPC Molecular Structure.....	21
11. DOTAP Molecular Structure.....	21
12. POPA Molecular Structure.....	21
13. Hydrophilic Drug Encapsulation of Liposomes.....	26
14. Unloaded Soy-PC/DOTAP SUV Size vs Sonication Time.....	31
15. Unloaded Soy-PC/DOTAP SUV Size vs Sonication Time.....	31
16. SEM Images of SUVs.....	35
17. Cytotoxicity of Media Dilutions.....	38
18. Cytotoxicity of Unloaded Soy-PC/DOTAP SUVs Normalized to Respective Media Dilutions.....	38
19. Cytotoxicity of Unloaded DOPC/POPA SUVs Normalized to Respective Media Dilutions.....	39

20. Cytotoxicity of Soy-PC/DOTAP SUVs Loaded with Curcumin .....	41
21. Cytotoxicity of DOPC/POPA SUVs Loaded with Curcumin.....	41
22. Cytotoxicity of Soy-PC/DOTAP SUVs Loaded with NAC.....	42
23. Cytotoxicity of DOPC/POPA SUVs Loaded with NAC.....	42
24. Cytotoxicity of Soy-PC/DOTAP SUVs Loaded with N-MPG.....	43
25. Cytotoxicity of DOPC/POPA SUVs Loaded with N-MPG.....	43
26. 48 Hour Lipid Hydroperoxidation.....	45
27. Pre-Incubation Images for Soy-PC/DOTAP SUVs.....	46
28. Pre-Incubation Images for DOPC/POPA SUVs.....	47
29. Peroxide Reduction of Soy-PC/DOTAP SUVs Loaded with Curcumin .....	48
30. Peroxide Reduction of DOPC/POPA SUVs Loaded with Curcumin.....	49
31. Peroxide Reduction of Soy-PC/DOTAP SUVs Loaded with NAC.....	50
32. Peroxide Reduction of DOPC/POPA SUVs Loaded with NAC.....	51
33. Peroxide Reduction of Soy-PC/DOTAP SUVs Loaded with N-MPG.....	52
34. Peroxide Reduction of DOPC/POPA SUVs Loaded with N-MPG.....	53

## I. INTRODUCTION

### 1.1 Background

Radiation exposure is both a major obstacle in space exploration and an occupational hazard for various careers. Radiation exposure can manifest itself as both immediate cell damage or as highly reactive oxygen free radicals[1]. The creation of energized reactive oxygen species (ROS) is the most well understood mechanism of radiation damage typically associated with low linear energy transfer (LET) radiation. These ROS will lead to the generation of highly reactive compounds that are shown to react with DNA bases and organelles[2]. This indirect mechanism can occur over time and has the additional potential to affect cells that have not been irradiated in what is known as the “Bystander Effect”[3]. High LET radiation can also cause the creation of ROS but due to its higher energy density, has the additional potential to directly cause DNA lesions (Figure 1) and damage in cellular organelles resulting in more immediate and more varied cell damage [4]. If radiation damage is unable to be repaired, it typically expresses itself as acute cell death or chronic cell dysregulations such as cancer.



Nature Reviews | Molecular Cell Biology

Figure 1: DNA Damage through Ionized Radiation and Antioxidant Benefit[5]

In order to reduce the effects of radiation, the primary and most explored approach has been focused around mitigation in terms of exposure duration, exposure intensity, and shielding usage. Since radiation is only directional in very controlled environments, exposure avoidance is frequently not a viable option. In addition, mitigating exposure time can still allow for significant radiation damage based on the intensity of the radiation and is not applicable in space and upper atmosphere operations. The most viable option to mitigate radiation in terms of received radiation reduction has been the use of shielding which comes with the requirement of high density materials which are frequently very expensive and can be a major detriment to any situation in which mobility is required. Specifically in the field of space exploration, the weight of shielding has a prohibitive effect on launch costs. An alternate approach to radiation

reduction is the use of supplements to mitigate the damage caused by the radiation received by the astronauts[6]. These supplements can be broadly named radioprotectants and are typically antioxidants[7]. Antioxidants function by eliminating ROS from the body and can prevent much of the long term damage and low LET radiation damage through ROS scavenging.

## 1.2 Antioxidants

One such antioxidant is curcumin (Figure 2), otherwise known as diferuloylmethane, is a component of turmeric with both antioxidant properties and anti-inflammatory properties. Curcumin is hydrophobic and soluble in acetone. The hydrophobic properties of curcumin's diketone group provide a ready location for hydrolysis and for ROS scavenging. In addition to the diketone group, the two phenolic hydroxyl groups have been shown to function as antioxidants as well (Figure 3). In addition to its ability to ROS scavenge, curcumin has been shown to up-regulate the expression of p53 which is identified as mediating DNA repair gene expression[8]. Curcumin also has the benefit of low toxicity; no toxic effects of oral doses of up to 8g daily after which point it was reported that consumption volume became the primary obstacle rather than toxicity. The very low oral toxicity is due in part to the low bioavailability of curcumin with peak serum levels after 1 hour being on the nanomolar scale[9]. The low blood serum levels of curcumin can be attributed to its rapid degradation and high liver clearance rate[10]. In physiological conditions, 90% of curcumin degradation has occurred in 30 minutes which is a severe limitation in its therapeutic use[11]. Because the primary mechanism for curcumin degradation is hydrolysis of the diketone moiety, the degradation of curcumin also removes a portion of



its antioxidant capabilities although some breakdown components retain antioxidant function (Figure 4).

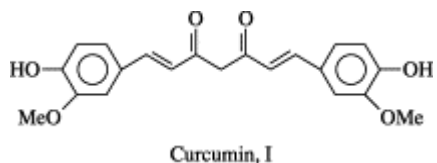


Figure 2: Curcumin Molecular Structure [12]

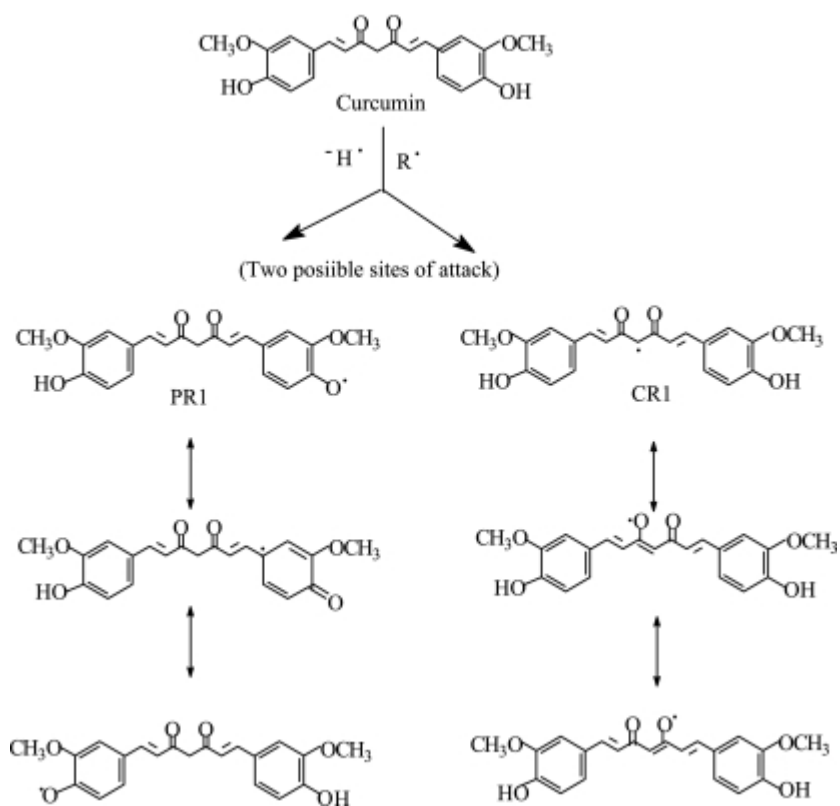


Figure 3: Reaction Pathway of Curcumin with Oxidizing Radicals[13]

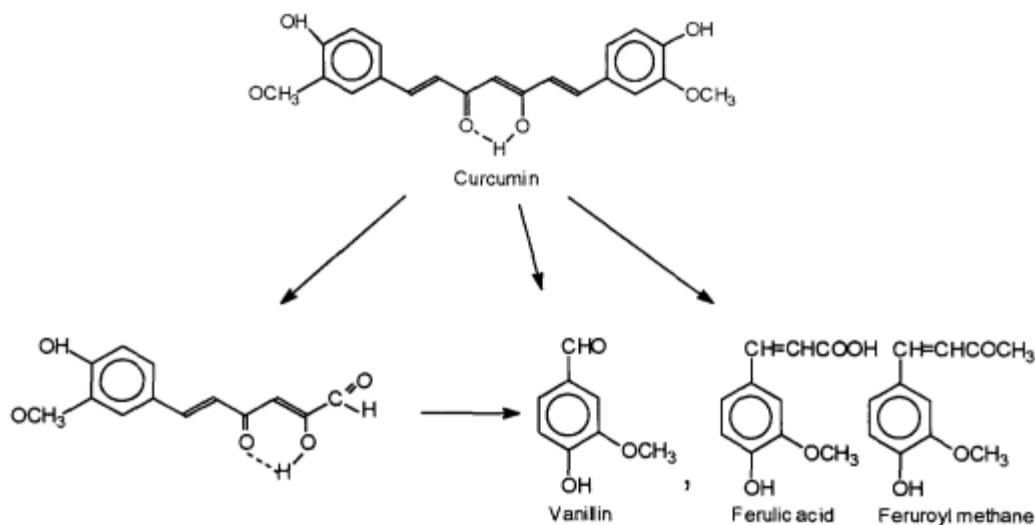


Figure 4: Curcumin Degradation Products[14]

Another antioxidant that could be used to scavenge free radicals, n-Acetylcysteine (NAC) (Figure 5) is both a pharmaceutical drug and a dietary supplement.

Pharmaceutically used to treat acetaminophen overdoses, NAC has received additional attention as a general health and bodybuilding supplement[15]. ROS scavenging for cysteines occurs through the formation of a disulfide bridge (Figure 6). Additionally NAC both up regulates and provides a precursor molecule (cysteine) to glutathione in the body which is an antioxidant and a regulatory signal for biological responses to ROS[16, 17]. However, disulfide bonds can form spontaneously when thiol groups are exposed to most oxidizing agents and therefore can reduce the efficacy of NAC as an antioxidant. A further challenge in the use of NAC is that it has a half-life of 1-2 hours in physiological conditions[18] which makes it difficult to maintain therapeutic concentrations of the antioxidants.

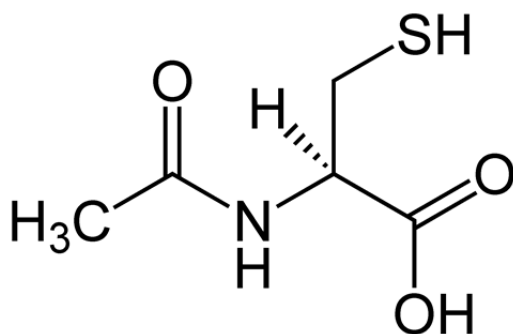


Figure 5: NAC Molecular Structure

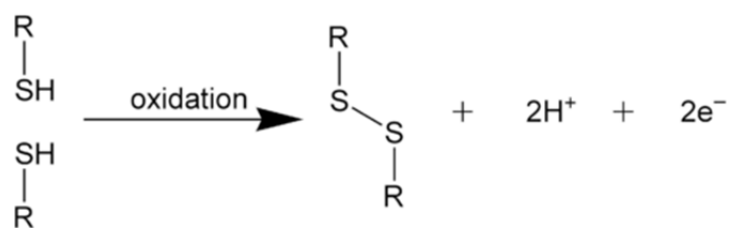


Figure 6: Disulfide Bridge Formation [19]

N-2-mercaptopropionyl glycine(N-MPG)(Figure 7), is also known as tiopronin and marketed under the trade name of Thiola® (Mission Pharmacal, San Antonio, Tx) in order to prevent the formation of kidney stones in patients who are resistant to diet modifications[20]. Like NAC, N-MPG has a thiol group with which antioxidant function stems from. N-MPG therefore, also functions as an antioxidant through the use of a disulfide bridge to reduce the effects of free radicals. Also like NAC, N-MPG suffers from a 1-2 hour half-life under physiological conditions which limits the therapeutic concentration that can be maintained[21].

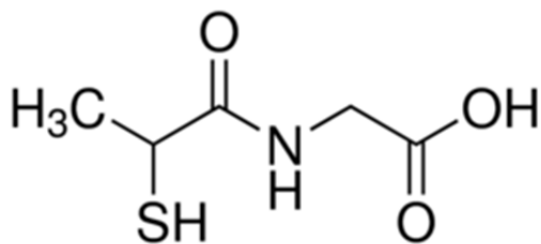


Figure 7: N-MPG Molecular Structure

### 1.3 Lipid Vesicles

Liposomes can be used to entrap materials such as NAC, N-MPG, and Curcumin. Liposomes can entrap hydrophobic molecules such as curcumin within the bilayer itself or hydrophilic materials such as NAC and N-MPG within the aqueous interior of the liposome[22]. Conventional liposome delivery of materials occurs through endocytosis and is limited by the rate at which this occurs[23]. Fusogenic liposomes fuse directly with the cell membrane to deliver materials rather than through endocytosis and can be used allow for faster, more consistent delivery of materials. Once entrapped, the lipid vesicles can be used to both protect its contents from outside degradation sources and subsequently as a delivery vehicle to deliver the entire contents of the vesicle to a cell by fusion. Lipid vesicles also have the ability to entrap hydrophobic molecules such as curcumin within the bilayer itself (Figure 8) which allows for the protection of curcumin from diketone hydrolysis, the primary mechanism of curcumin degradation, in addition to allowing full delivery of curcumin into target cells upon vesicle fusion[24].

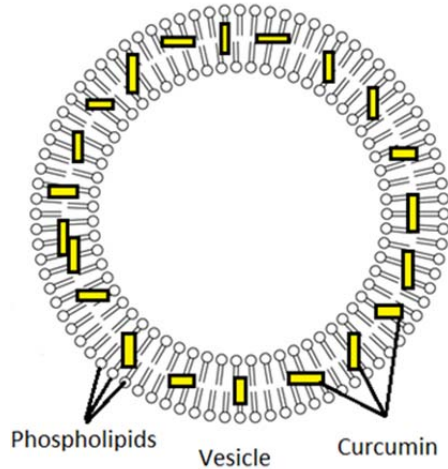


Figure 8: Curcumin Containing Lipid Vesicle[25]

Two different liposome compositions were studied. The first composition was Soy-Phosphatidylcholine (Soy-PC) and 1,2-dioleoyl-3-trimethylammonium-propane (DOTAP) (50:1 mol/mol respectively) and the second composition was 1,2-dioleoyl-*sn*-glycero-3-phosphocholine (DOPC) and 1-palmitoyl-2-oleoyl-*sn*-glycero-3-phosphate (POPA) (50:1 mol/mol respectively)[26]. Soy-PC (Figure 9) and DOPC (Figure 10) are act as stable vesicle formers that comprise the majority of the liposomes and provide stability to the vesicles formed. Soy-PC is actually a heterogeneous mixture of phosphatidylcholines of which the most common species is shown in figure 9. DOTAP (Figure 11) is a cationic lipid and POPA (Figure 12) is an anionic phospholipid both of which are unstable vesicle formers used to impart fusogenic properties to vesicles.

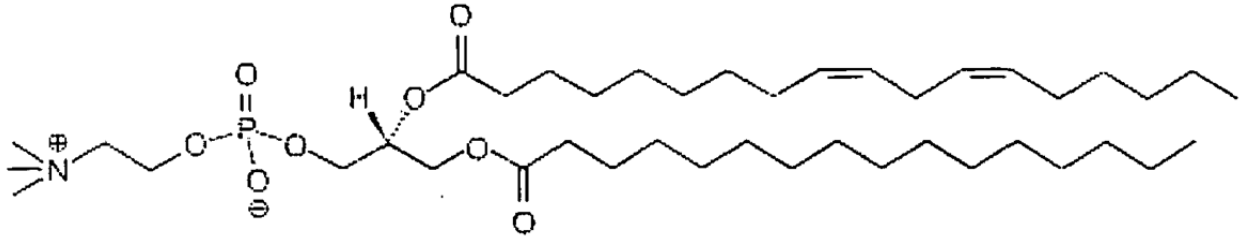


Figure 9: Soy-PC Primary Species Molecular Structure[26]

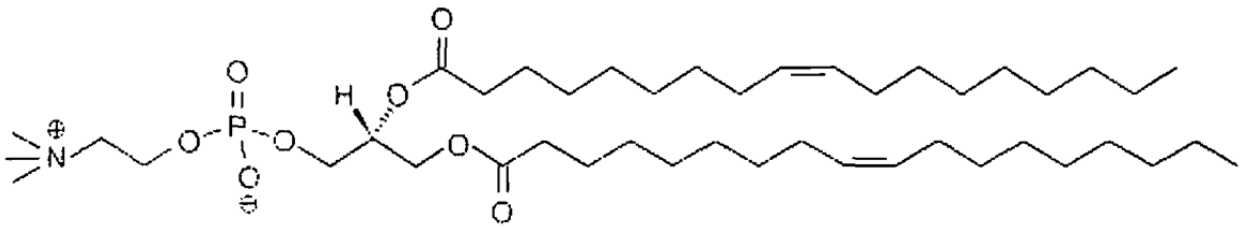


Figure 10: DOPC Molecular Structure[26]

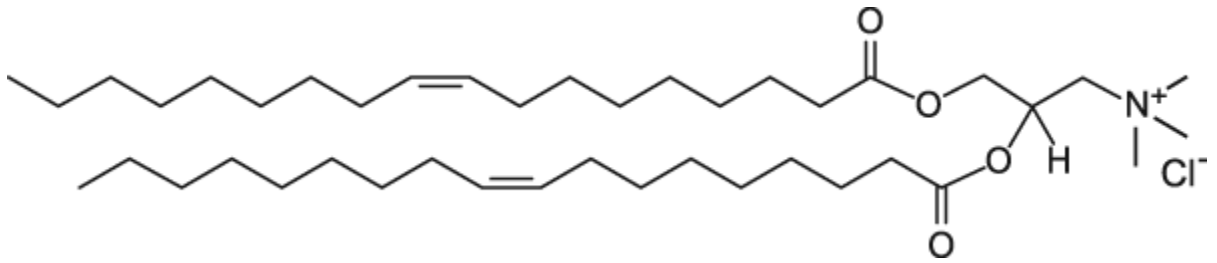


Figure 11: DOTAP Molecular Structure[27]

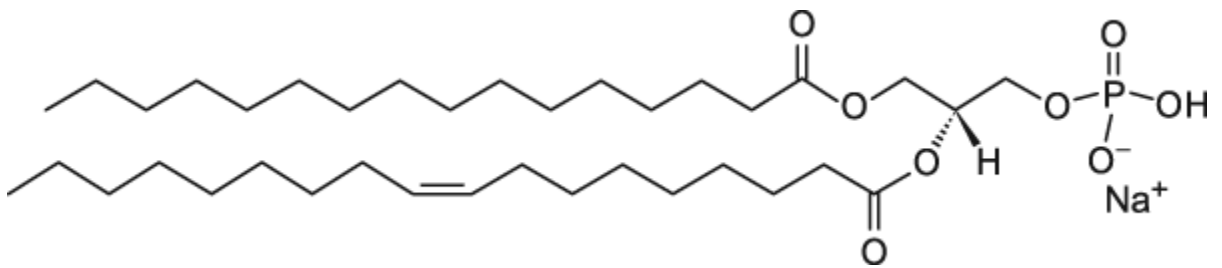


Figure 12: POPA Molecular Structure[27]

While lipid vesicles spontaneously form upon rehydration, their formation will occur in varying sizes and with a varied number of bilayers. In order to create unilamellar vesicles of consistent sizes, high stress mixing methods such as sonication, emulsification, and homogenization must be used[28]. For small batch development (<10 mL), probe sonication is the most applicable and will be used to create unilamellar vesicles for testing. The sonication process used here creates small unilamellar vesicles (SUVs) that were at their limiting hydrodynamic radius.

#### 1.4 Hypothesis

Antioxidant loaded SUVs can be fabricated via probe sonication and maintain antioxidant function without an increase in cytotoxicity while increasing cellular uptake of the antioxidants and decrease ROS levels in human dermal fibroblasts.

## II. METHODS

### 2.1 Small Unilamellar Vesicle (SUV) Fabrication

SUV synthesis by sonication involves two phases, a drying phase to remove the chloroform solvent and a rehydration phase to hydrate the lipid material. For the drying phase, 5 mg (125  $\mu$ l at 40 mg/ml) of Soy-PC (Avanti, Birmingham, AL) and 0.090 mg (36.6  $\mu$ l at 2.5 mg/ml) of DOTAP (Avanti) were added to a test tube. A second lipid composition of 5 mg (200  $\mu$ l at 25 mg/ml) DOPC (Avanti) and 0.089 mg (35.4  $\mu$ l at 2.5 mg/ml) of POPA (Avanti) was also examined for comparative purposes in this study. Chloroform was the solvent for all lipids.

For testing conditions that required the addition of curcumin (Sabinsa), the curcumin was dissolved in acetone and added into the lipid solution. The amount of curcumin at a 1:10, 1:50 and 1:100 molar ratio of (curcumin: lipid) and labelled as 10%, 2%, and 1% curcumin loading respectively. 10% curcumin can also be considered as 130.4 $\mu$ M. Once the components were added into the test tube, a stream of nitrogen gas was then used to evaporate off the solvents. Once dried, the remaining lipid residue was light protected and placed under vacuum storage (Thermo, Air Cadet) for a minimum of 12 hours to ensure removal of trace amounts of solvent.

For the rehydration phase, the lipid residue was suspended in 5 mL of Hank's Balanced Salt Solution (HBSS) (Sigma, St. Louis, MO) and 10 mM Trizma base (Sigma) at pH 7.4. NAC (Sigma) and N-MPG (Sigma) concentrations were calculated relative to their solvent (water) and therefore 10% NAC and 10% N-MPG were 0.1 mg/mL. For both NAC and N-MPG, 10% can also be considered 612 $\mu$ M. For a given 5 mL sample of



10% NAC/N-MPG, 0.5 mg of NAC/N-MPG was added to the lipid suspension. Two 5mm glass beads (Sigma) were then added to assist in removal of the lipid residue from the test tube surface. The test tubes were parafilmmed and vortexed for 30 seconds then placed in a 37<sup>0</sup>C water bath for 1 hour. During the hour in the water bath, the samples were vortexed for 30 seconds every 15 minutes to ensure complete hydration of the sample. After the water bath, the samples were then transferred to 15 mL centrifuge tubes and probe sonicated (Branson, Sonifier 450) with a booster horn and micro-tip probe at 50% duty cycle and an output control of 7 (micro-tip limit). Sonication was continued until the limiting hydrodynamic radius was reached. The limiting particle radius was considered to be the size where there was no longer a significant reduction in SUV diameter with additional sonication time. To assist in keeping sonication parameters consistent over multiple batches, the samples were kept in a cold water bath (16<sup>0</sup>C-18<sup>0</sup>C) and the probe was placed both centrally and as deep as possible without causing cavitation of the suspended sample. The samples were then centrifuged at 3100 rpm (Beckman, TJ-6) for 5 minutes to remove titanium particles that erode from the sonicator tip during use. Samples were then transferred to another centrifuge tube without disturbing the pellet and analyzed by DLS (Wyatt, DynaPro) for average diameter and polydispersity. The software package Dynamics V6 was used in conjunction with the DLS. Samples were then, capped, protected from light, and stored at 4<sup>0</sup>C until use within 1 day of production.

## 2.2 Dynamic Light Scattering (DLS) analysis

Each SUV sample was analyzed by DLS (Wyatt, DynaPro) in order to determine the hydrodynamic radius of the SUVs. Hydrodynamic radius is a measure of particle size

calculated from particle diffusion rates based on the Stokes-Einstein equation[29]. DLS size calculations were performed at room temperature and based on a preprogrammed model for globular proteins. A minimum of 50 readings per sample was taken for all samples which were analyzed immediately after liposome production with a minimum intensity of 20,000 cnts/mL. The metrics of mean diameter, diameter standard deviation, and sample polydispersity were noted for each sample.

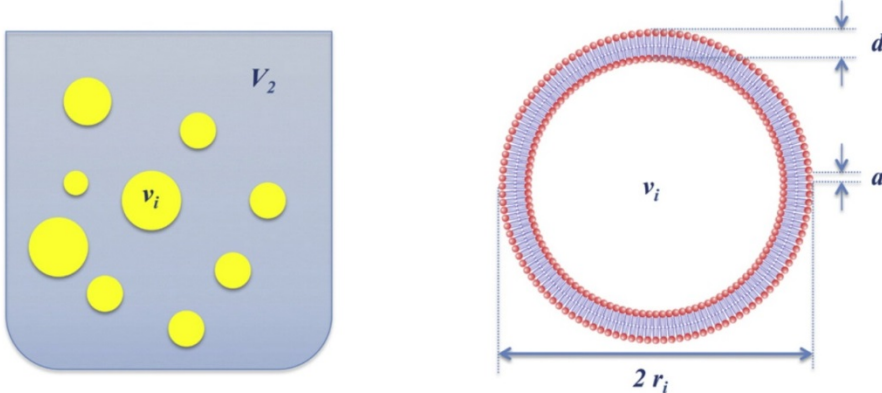
### 2.3 SEM Imaging

In order to examine SUV morphology, 5 $\mu$ L of sample was placed on a silicon wafer, covered, and allowed to air dry at room temperature for a minimum of 12 hours. The silicon wafers were then placed on copper stubs and were imaged by SEM (Zeiss Evo, 3.22 kV, InLens detector). Images were able to be obtained without sputter coating for Soy-PC/DOTAP liposomes and DOPC/POPA samples required sputter coating for 1 minute using gold/palladium with parameters of 150 V, 0.1 mA, and under a 0.1 torr vacuum. For both SUV compositions, unloaded samples and samples loaded at 10% concentrations were analyzed for morphological changes since any morphological changes that occurred at 1% and 2% loading conditions were expected to be similar to 10% loading but much harder to visualize.

### 2.4 Theoretical Loading Efficiency of SUVs

Because of the difficulty separating SUVs from solution, theoretical loading efficiency was determined to estimate the amount of antioxidant contained within the SUVs. For curcumin, because it was not water soluble and was trapped within the lipid bilayer prior to rehydration, loading efficiency was considered to be at or very near 100%

for both SUV compositions. For NAC and N-MPG, loading was expected to follow the model of hydrophilic drug entrapment for SUVs. Hydrophilic antioxidant encapsulation efficiency was calculated according to the equation in Figure 13. The encapsulation efficiency equation takes the metrics of particle size, standard deviation, bilayer thickness, molecular polar surface area, lipid concentration, and sample volume to estimate the percentage of antioxidant encapsulated. The encapsulation efficiency equation can be broken down into inner volume ( $V_i$ ), vesicle count, and total sample (outer) volume ( $V$ ). Inner volume was determined as a function of radius ( $R_i$ ) and bilayer thickness ( $d$ ). Vesicle count was determined by the lipid concentration ( $C$ ) and the number of lipid molecules per vesicle ( $N_A$ ) was based on bilayer surface area and the exposed area of a single lipid molecule ( $a$ ). This calculation was then repeated with probability weights ( $P_i$ ) over a log normal distribution vesicle sizes. Based on the encapsulation efficiency equation, the hydrophilic encapsulation efficiency for Soy-PC/DOTAP and DOPC/POPA SUVs were 0.88% and 0.90% respectively.



$$EE\% = \frac{V_m}{V} \times 100\% = \frac{\sum_i \left( \frac{4}{3} \pi (r_i - d)^3 \cdot \frac{c \cdot V \cdot N_A}{\sum_i \left( \frac{4\pi [r_i^2 + (r_i - d)^2] \cdot P_i}{a} \right) \cdot P_i} \right)}{V} \times 100\%$$

$EE\% \propto c, r, a, -d$

Figure 13: Hydrophilic Drug Encapsulation of Liposomes[22]

## 2.5 Human Dermal Fibroblast (HDF) cell culture

All cell based analysis was performed with human dermal fibroblasts (HDF). HDF passage number was not allowed above 20. HDFs were cultured in RPMI 1640 (Thermo, Waltham, MA) with 10% fetal bovine serum (Thermo) and 1% penicillin-streptomycin (Thermo). HDFs cultured in 96 well plates were given 100  $\mu$ L of media and those cultured in 48 well plates were given 250  $\mu$ L of media. Cell seeding densities were 10,000 cells per well for 96 well plates and 30,000 cells per well for 48 well plates and all experiments were performed at full confluence.

## 2.6 Cellular Uptake of Curcumin from SUVs

SUV delivery of antioxidants was estimated based on cellular curcumin uptake in HDFs. Curcumin is naturally fluorescent in the green spectrum (Ex at 420 nm and Em at 470 nm) and therefore can be visualized with a FITC filter on a fluorescent microscope (Nikon, Eclipse Ti). Curcumin uptake was examined visually to determine pre-incubation times for future cell based assays

## 2.7 MTT Assay for Cytotoxicity

Cytotoxicity assays for all conditions were performed in 96 well plates on confluent HDFs. Promega's CellTiter 96 Non-Radioactive Cell Proliferation Assay kit (Promega, Madison, WI) was used to assess cellular viability after 24 hours of SUV treatments. All treatment conditions and controls were removed, washed with phosphate buffered saline (Thermo), and given fresh media after 24 hours of treatment time immediately before performing the MTT assay. The formazan forming tetrazolium dye was incubated at 37  $^{\circ}$ C protected from light for 2 hours and the stop solution was

incubated protected from light at room temperature for on an orbital rocker (Barnstead, model# 4631) for 1 hour. All observed bubbles were then removed from each sample and the absorbance was read on a plate spectrophotometer at 562 nm (BioTek, ELx800).

### 2.8 Lipid Hydroperoxidation

As a precursor assay to the measurement of antioxidant capacity, lipid hydroperoxidation measurements were required to obtain the amount of peroxides produced by the SUV degradation. These measurements were taken using the PeroxiDetect Kit (Sigma). A stock of 90% methanol was created by 108 mL of methanol with 12 mL water. A stock solution of Organic Peroxide Color Reagent was created by reconstituting the entire contents of the kit stock bottle in 120 mL of 90% methanol. A Working Color Reagent was then created by adding 100 volumes of the reconstituted Organic Color Reagent to 1 volume of Ferrous Ammonium Sulfate Reagent. Then 100  $\mu$ L of sample was placed into a cuvette to which 1 mL of the Working Color Reagent was added. The samples were then protected from light and incubated at room temperature for 30 minutes. Samples absorbance was then measured by a spectrophotometer (Thermo) at 560 nm. A standard curve was created using tert-butyl hydroperoxide as a positive control without lipids.

### 2.9 Antioxidant Capacity

The antioxidant capacity of the samples given to HDFs was determined using an Amplex Red hydrogen peroxide assay kit from Invitrogen. The Amplex Red assay was performed in a 48 well plate on confluent HDFs and requires the use of RPMI 1640 without phenol red with 25 mM HEPES (Calbiochem, San Diego, CA) and 1%

penicillin-streptomycin (Sigma). Prior to performing the assay, stock solutions of reaction buffer, horseradish peroxidase (HRP), and Amplex Red (Cayman) were created. The reaction buffer was 25 mL of 50 mM sodium phosphate at pH 7.4. The HRP stock solution (Invitrogen) was dissolved in reaction buffer at 10 U/mL and divided into 120  $\mu$ L aliquots for future use. The Amplex Red stock solution was dissolved into DMSO (Sigma) at 390  $\mu$ L/mg and then divided into 60  $\mu$ L aliquots. SUV blank controls, free antioxidant controls, and antioxidant loaded SUVs were added with fresh media and given a 20 minute pre-incubation time at 37  $^{\circ}$ C. After the pre-incubation time, 125  $\mu$ L of 100  $\mu$ M hydrogen peroxide (Sigma) was added to the relevant samples and allowed to incubate at 37  $^{\circ}$ C for 10 minutes. A stock of working Amplex Red was then made by mixing 50  $\mu$ L of an Amplex Red aliquot, 100  $\mu$ L of an HRP aliquot, and 2.42 mL of reaction buffer. Next, 125  $\mu$ L of working Amplex Red was then added to all samples and allowed incubate at 37  $^{\circ}$ C for 1 hour. After the addition of both the hydrogen peroxide and the Amplex Red, the final concentrations of both the Amplex Red and hydrogen peroxide dilute to 25  $\mu$ M. The absorbance was read on a plate spectrophotometer (BioTek, ELx800) at 562 nm.

### III. RESULTS

#### 3.1 SUV Size Analysis and Production

Because SUVs naturally form over a range of sizes, forcing SUVs towards the limiting hydrodynamic radius was necessary to produce a batch of SUVs with consistent vesicle size. Initial samples for both Soy-PC/DOTAP and DOPC/POPA SUVs (Figures 14 and 15) showed that sonication does force SUV size towards the limiting hydrodynamic radius. In addition, the sonication times at which the limiting hydrodynamic radius was being approached for both Soy PC-DOTAP and DOPC/POPA SUVs were 3 to 4 minutes. A change of SUV diameter of less than 10% was used as a metric to determine that the SUV size was approaching the limiting hydrodynamic radius after which further sonication would not cause significant size reduction. Therefore, additional analysis began with multiple samples at 3 minutes of sonication time.

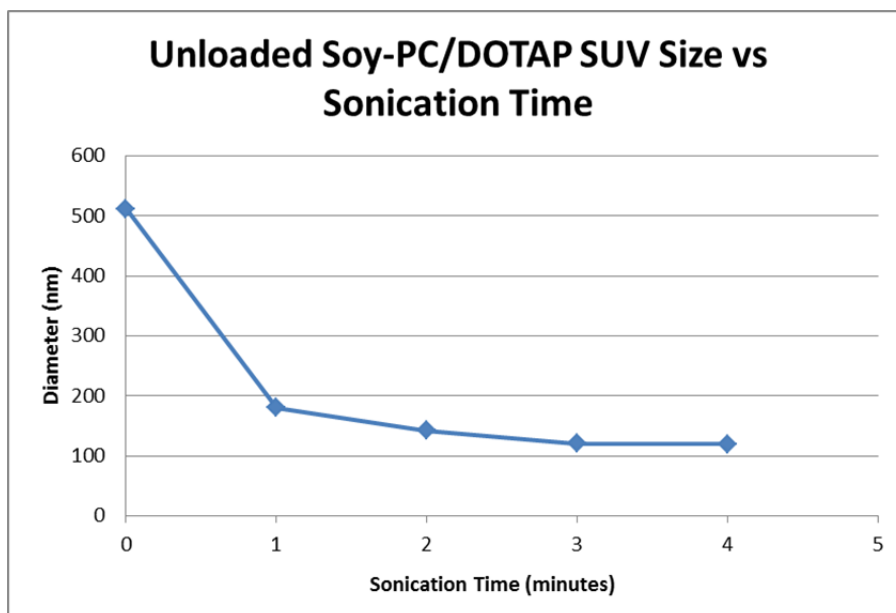


Figure 14: Unloaded Soy-PC/DOTAP SUV Size vs Sonication Time. Less than 10% size change occurred between 3 and 4 minutes of sonication time.

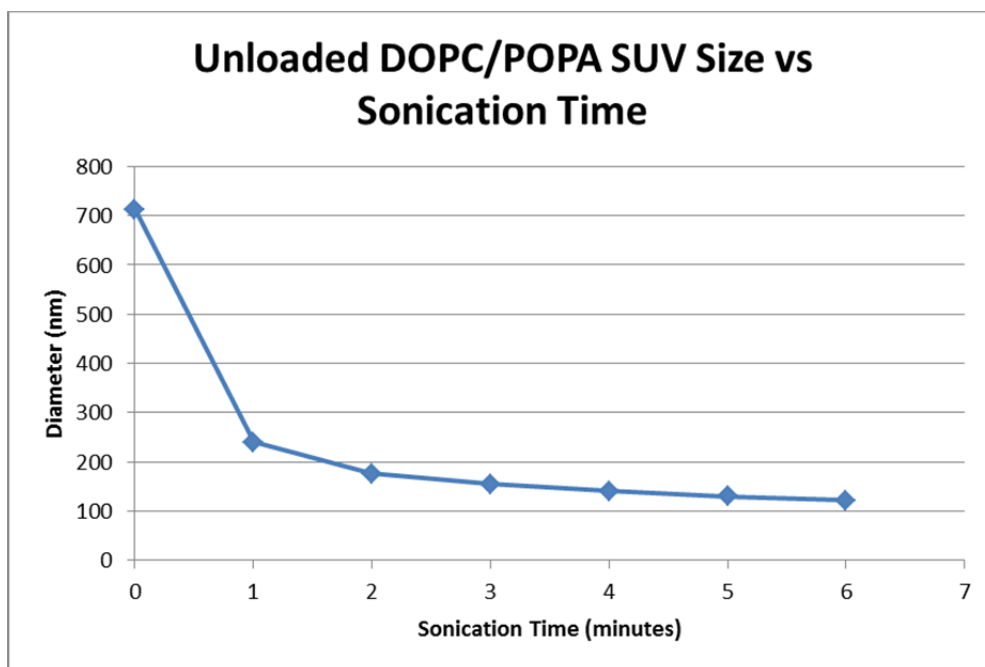


Figure 15. Unloaded Soy-PC/DOTAP SUV Size vs Sonication Time. Less than 10% size change occurred between 3 and 4 minutes of sonication time.



SUV size analysis was used to determine if the limiting hydrodynamic radius had been reached for all conditions at the sonication times indicated by the estimates provided by Figures 14 and 15. If the mean SUV size was not statistically different between 2 sonication times, the limiting hydrodynamic radius had been achieved. The results of tables 1 and 2 showed that the limiting hydrodynamic radius had been reached between 3 and 4 minutes for all conditions except for sdn10, dpc10, dpcn2, and dpcn10. A high curcumin concentration, such as dpc10, will interfere with lipid formation until even dispersion throughout the lipid bilayers is achieved through further sonication. The results of table 3 show that the limiting hydrodynamic radius had been reached for sdn10, dpc10, and dpcn2 in between 4 minutes and 5 minutes of sonication time. Table 3 also showed that the limiting hydrodynamic radius had been reached for dpcn10 in between 5 minutes and 6 minutes of sonication time. Based on these results, the production times of each SUV condition for further studies were placed halfway in between the times in which the limiting hydrodynamic radius had been reached and the sizes of which are shown in Table 4.

	sd0	sdc1	sdc2	sdc10	sdm1
3 minutes	122.1 ± 1.6	126.2 ± 3.5	120.1 ± 4.6	124.5 ± 2.7	126.7 ± 3.8
4 minutes	115.1 ± 4.0	113.9 ± 9.9	111.5 ± 6.7	115.7 ± 4.3	117.8 ± 9.1
significant diff.	no	no	no	no	no
	sdm2	sdm10	sdn1	sdn2	sdn10
3 minutes	126.8 ± 5.7	129.0 ± 3.2	122.6 ± 3.2	127.2 ± 6.4	123.4 ± 4.0
4 minutes	117.4 ± 8.5	113.5 ± 6.7	117.8 ± 1.7	116.8 ± 1.3	113.0 ± 2.9
significant diff.	no	no	no	no	yes

Table 1: Size Analysis of Mean Diameter vs Sonication Times for Soy-PC/DOTAP SUVs. Table shows that only sdn10 had a significant size difference between 3 and 4 minutes as shown by t-tests,  $p=0.05$ ,  $n=3$

	dp0	dpc1	dpc2	dpc10	dpm1
3minutes	143.8 ± 10.0	150.8 ± 2.0	149.0 ± 5.6	*	146.2 ± 6.7
4minutes	130.4 ± 9.1	137.5 ± 4.3	132.5 ± 2.9	129.0 ± 2.8	131.0 ± 3.8
significant dif.	no	no	no	n/a	no
	dpm2	dpm10	dpn1	dpn2	dpn10
3minutes	145.3 ± 4.0	145.8 ± 3.0	144.0 ± 3.5	140.8 ± 2.7	142.8 ± 1.1
4minutes	133.8 ± 1.0	130.6 ± 5.0	130.7 ± 4.0	127.6 ± 1.9	129.6 ± 1.8
significant dif.	no	no	no	yes	yes

Table 2: Size Analysis of Mean Diameter vs Sonication Times for DOPC/POPA SUVs. Table shows that only dpn2 and dpn10 had a significant size difference between 3 and 4 minutes as shown by t-tests,  $p=0.05$ ,  $n=3$

\*Lipid precipitate observed at dpc10 3 minutes therefore sample was not viable due to unknown lipid concentrations of supernatant

	sdn10	dpc10	dpn2	dpn10		dpn10
4minutes	113.0 ± 2.9	129.0 ± 2.8	127.6 ± 1.9	129.6 ± 1.8	5minutes	121.0 ± 1.6
5minutes	108.1 ± 4.5	119.6 ± 2.0	124.8 ± 1.8	121.0 ± 1.6	6minutes	117.8 ± 1.1
significant dif.	no	no	no	yes	significant dif.	no

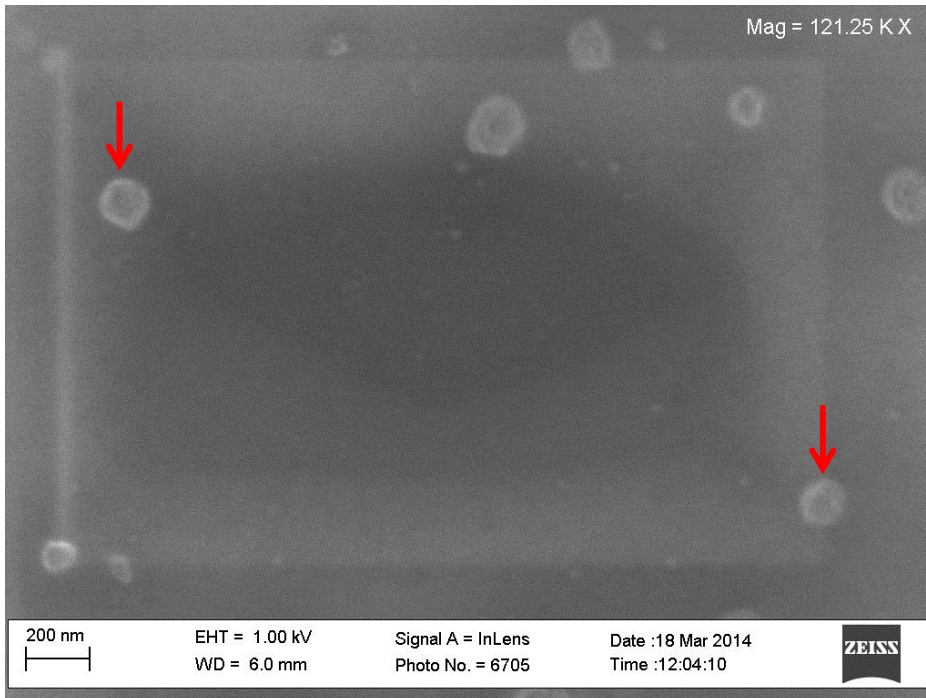
Table 3: Size Analysis of Mean Diameter vs Sonication Times for Extended Sonication Times. Table shows that only dpn10 had a significant size difference between 4 and 5 minutes as shown by t-tests,  $p=0.05$ ,  $n=3$

sd0	sdc1	sdc2	sdc10	sdn1	sdn2	sdn10	sdm1	sdm2	sdm10
123.3±8.3	125.0±8.8	125.5±7.0	118.5±6.6	125.0±7.6	125.3±6.7	121.5±6.1	123.6±5.5	127.2±7.7	125.5±8.5
dp0	dpc1	dpc2	dpc10	dpn1	dpn2	dpn10	dpm1	dpm2	dpm10
134.1±7.9	140.2±0.6	138.6±5.0	131.2±5.0	140.0±0.8	124.2±4.8	119.0±3.3	141.4±0.0	139.3±0.4	140.7±4.9

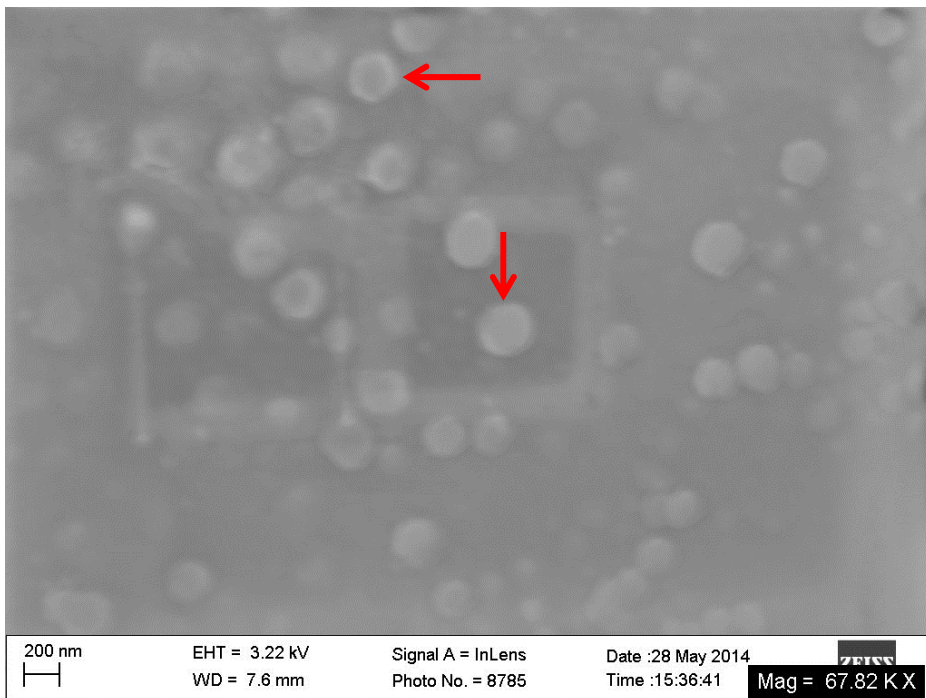
Table 4: SUV Sizes at Production Sonication Times. Table shows the average SUV size (nm) ± the standard deviation. All conditions have  $n \geq 3$  other than dpn and dpm loading conditions ( $n=2$ ).

### 3.2 SUV Characterization by SEM

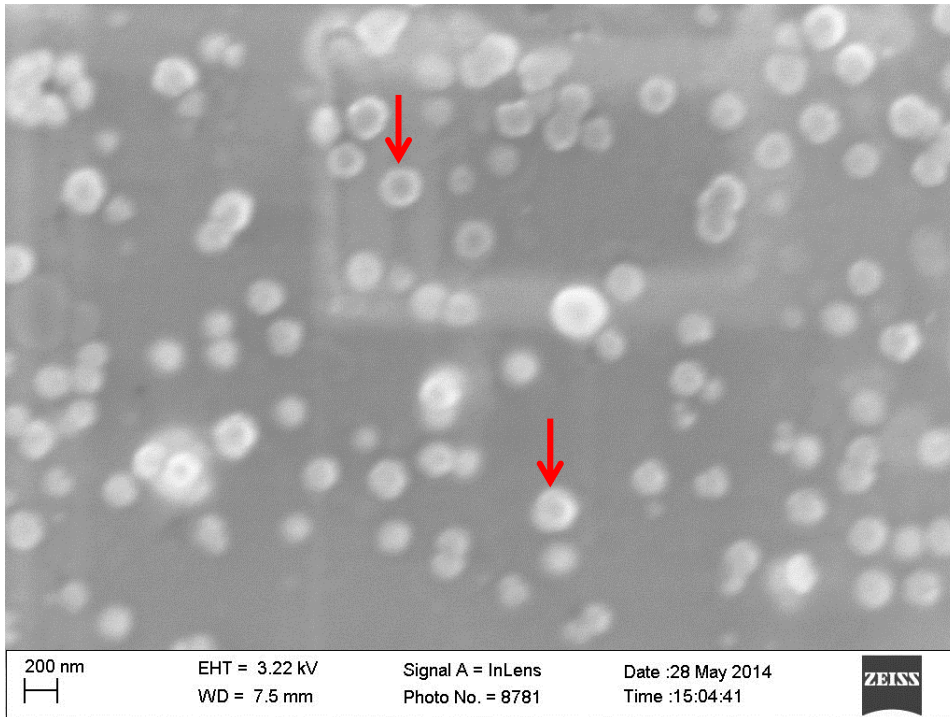
SEM microscopy of SUV samples showed that all imaged Soy-PC/DOTAP SUV samples had a consistently unilamellar and spherical morphology. DOPC/POPA SUVs were much more difficult to image most likely due to the lack of charge provided by the cationic lipid DOTAP and only one out of the 4 conditions attempted were able to be imaged. DOPC/POPA SUV morphology appears to be unilamellar but less spherical than the Soy-PC/DOTAP SUVs. For the Soy-PC/DOTAP SUVs, the images shown were collected without the use of sputter coating. For DOPC/POPA, SUVs needed to be sputter coated to obtain images. DLS size measurements were considered to be a better representation of SUV size because DLS measurements were taken while SUVs were still hydrated and the effects of dehydrating the SUVs for SEM imaging were unknown.



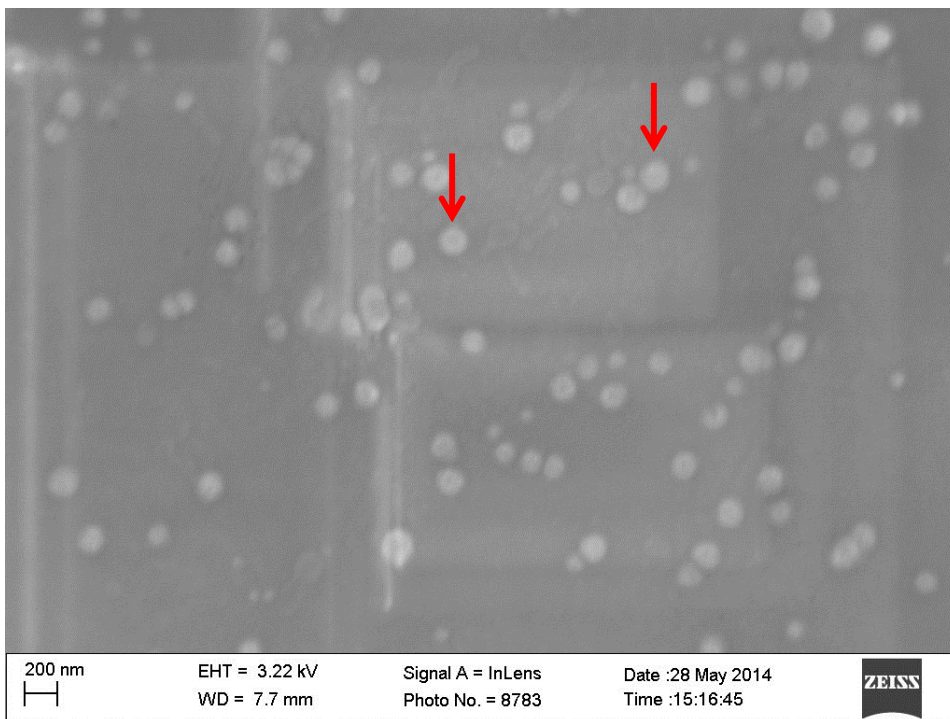
Panel A: Soy-PC/DOTAP Unloaded SUVs



Panel B: Soy-PC/DOTAP SUVs Loaded with 10% Curcumin

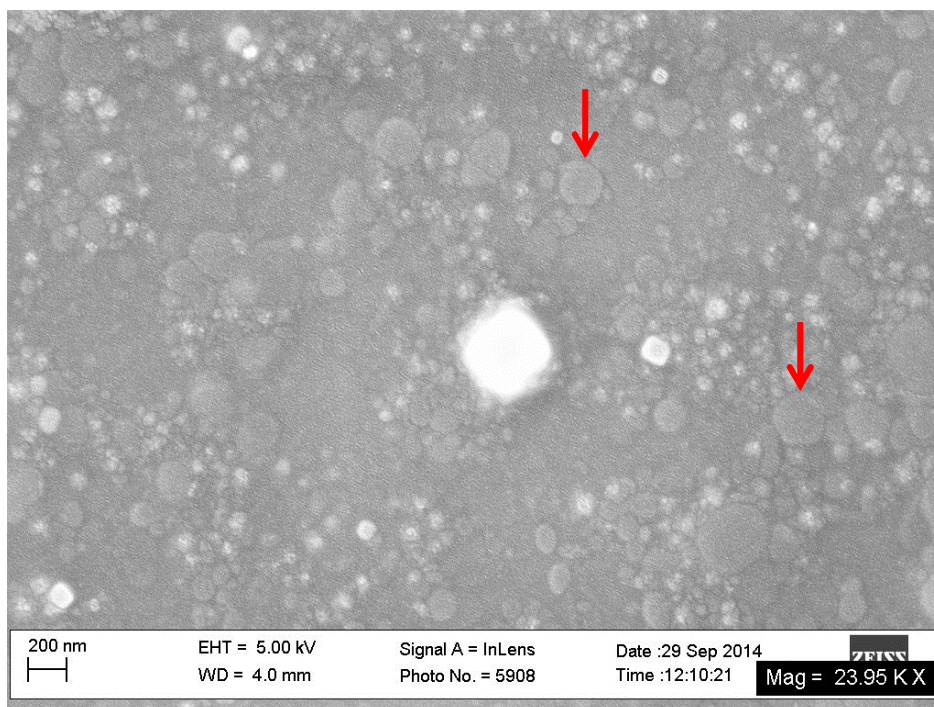


Panel C: Soy-PC/DOTAP SUVs Loaded with 10% Curcumin



Panel D: Soy-PC/DOTAP SUVs Loaded with 10% N-MPG





Panel E: DOPC/POPA SUVs Loaded with N-MPG

Figure 16 A-E: SEM Images of SUVs. All SUVs appear to be unilamellar and round.

### 3.3 SUV Cytotoxicity

Because the SUVs are rehydrated and sonicated in HBSS and Trizma Base, adding the SUVs to media for cell studies dilutes the media and subsequent nutrients. Therefore before the cytotoxicity of the SUVs could be studied, the cytotoxicity of the media dilutions needed to be established. The results of Figure 17 show that media that is 50% HBSS and Trizma base or greater caused significant cytotoxicity. Therefore the media that was 25% HBSS and Trizma base would be the maximum concentration of SUVs used in cell studies.

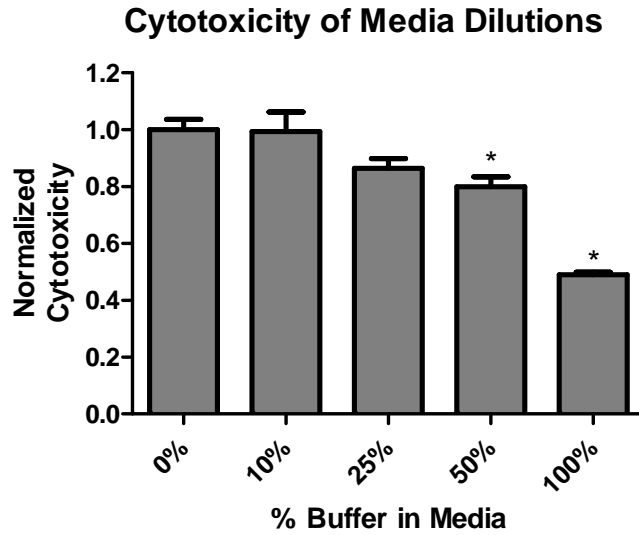


Figure 17: Cytotoxicity of Media Dilutions (Note: Buffer is HBSS and 10mM Trizma base). Significant cytotoxicity differences are noted with \* at 50% and 100% buffer in media as tested by ANOVA,  $p < 0.05$ ,  $n = 5$ , and with Tukey's post test.

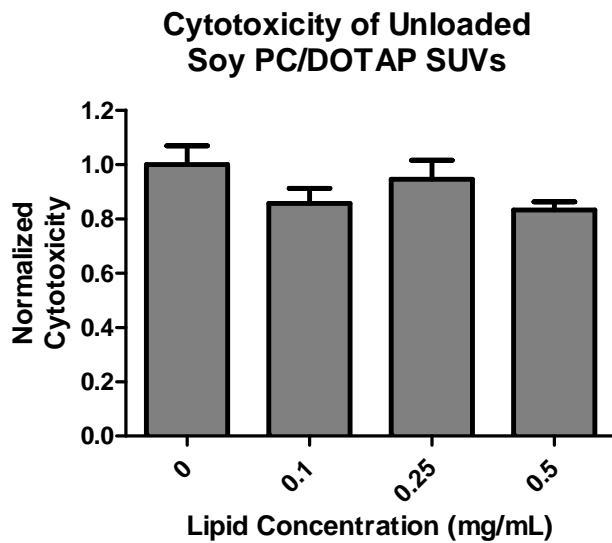


Figure 18: Cytotoxicity of Unloaded Soy-PC/DOTAP SUVs Normalized to Respective Media Dilutions. No significant cytotoxic effects were seen as tested by ANOVA,  $p < 0.05$ ,  $n = 5$ , and with Tukey's post test.

Unloaded SUV cytotoxicity was needed to establish the maximum concentration of SUVs that could be used to treat HDFs. The results in Figure 18 and Figure 19 indicate that there was no significant toxicity in either of the SUV compositions for all concentrations when compared to their respective controls of equivalent media conditions. Because the SUV batches were produced at a concentration of 1 mg/mL in buffer, the fraction of media that was buffer can be correlated directly to the lipid concentration (e.g. 0.25 mg/mL SUV had a respective control of media that was 25% buffer). Neither SUV composition was cytotoxic to the HDFs and thus both SUV compositions were used at 0.25 mg/mL for future studies.

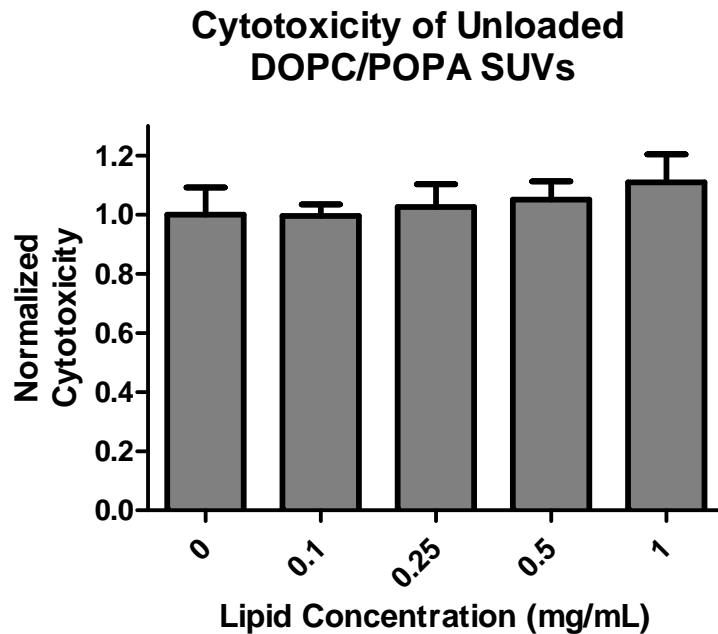


Fig 19: Cytotoxicity of Unloaded DOPC/POPA SUVs Normalized to Respective Media Dilutions. No significant cytotoxic effects were seen as tested by ANOVA,  $p < 0.05$ ,  $n = 5$ , and with Tukey's post test



Loaded SUV cytotoxicity was investigated to determine if the concentrations of antioxidants being used were cytotoxic to HDFs. Because of the lipid dilutions due to the cytotoxicity results of unloaded SUVs, loaded SUV molarities are reduced to 32.6 $\mu$ M for curcumin and 153 $\mu$ M for NAC/N-MPG. The results shown in Figures 20, 21, and 22 show that there were no significant cytotoxic effects of the antioxidants on HDFs. This data indicates that all tested concentrations of antioxidants can continue to be evaluated without significant toxic effects to the HDFs. Previous unpublished data by our group indicated that neither free NAC nor free N-MPG would have significant cytotoxic effects at the concentrations that were tested in the MTT assay. Our group has previously shown that curcumin would be cytotoxic above 10  $\mu$ M which was below the concentration of curcumin used (32.6  $\mu$ M). The discrepancy between toxicity levels shown in Figure 20 and the previous lab data could be attributed to the curcumin being obtained from Sabinsa while curcumin for previous data was obtained from Sigma. Another possible reason for the curcumin toxicity discrepancy is that while not significant, the reduced HDF metabolism caused by the 25% media dilution could reduce the amount of toxic byproducts of curcumin metabolism. A third possibility is that a portion of the curcumin was not released if the SUVs had not had a chance to fuse with the cells although given that the study took place over the course of 24 hours, it is expected that the fraction of unfused SUVs remains very small. While not significant, DOPC/POPA SUVs showed a lower toxicity than the Soy-PC/DOTAP SUVs and free antioxidants.

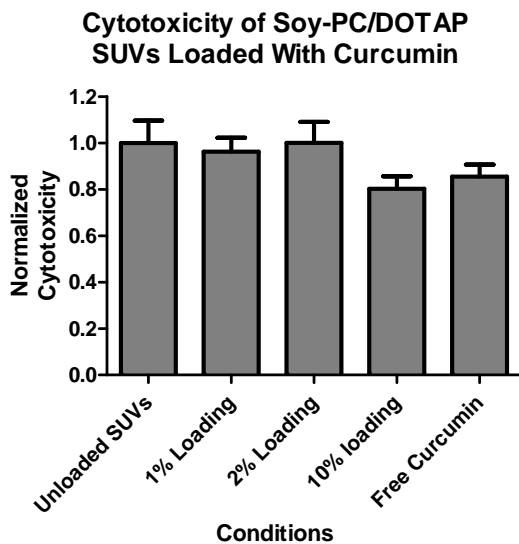


Figure 20: Cytotoxicity of Soy-PC/DOTAP SUVs Loaded with Curcumin. No significant cytotoxic effects were seen as tested by ANOVA,  $p < 0.05$ ,  $n = 5$ , and with Tukey's post test.

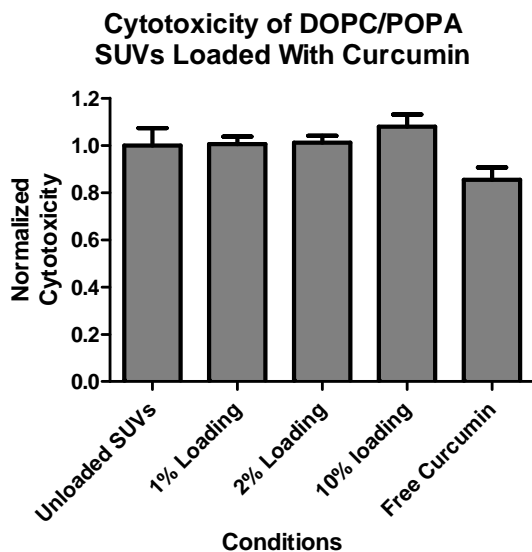


Figure 21: Cytotoxicity of DOPC/POPA SUVs Loaded with Curcumin. No significant cytotoxic effects were seen as tested by ANOVA,  $p < 0.05$ ,  $n = 5$ , and with Tukey's post test.

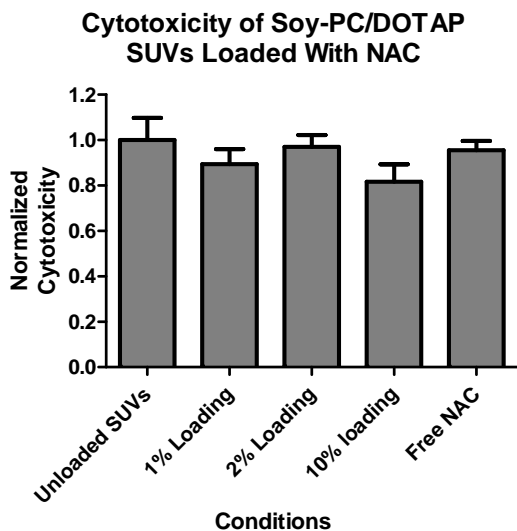


Figure 22: Cytotoxicity of Soy-PC/DOTAP SUVs Loaded with NAC. No significant cytotoxic effects were seen as tested by ANOVA,  $p < 0.05$ ,  $n = 5$ , and with Tukey's post test.

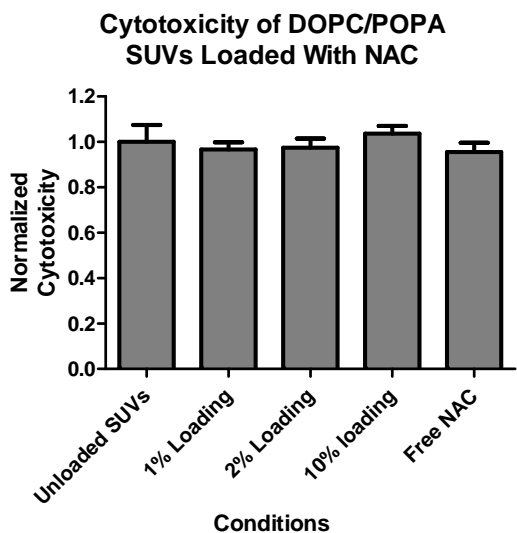


Figure 23: Cytotoxicity of DOPC/POPA SUVs Loaded with NAC. No significant cytotoxic effects were seen as tested by ANOVA,  $p < 0.05$ ,  $n = 5$ , and with Tukey's post test.

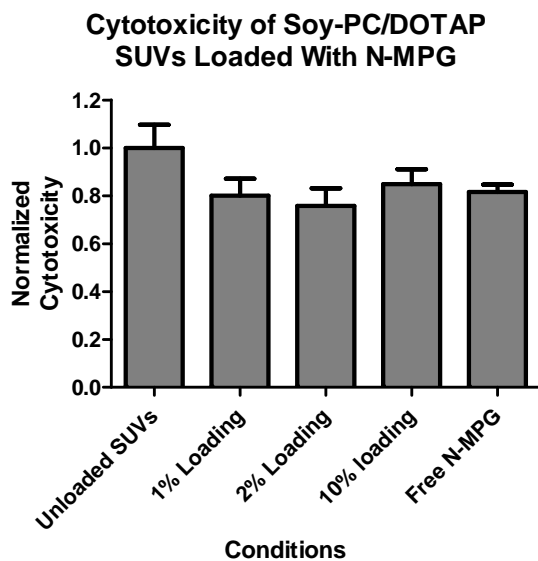


Figure 24: Cytotoxicity of Soy-PC/DOTAP SUVs Loaded with N-MPG. No significant cytotoxic effects were seen as tested by ANOVA,  $p < 0.05$ ,  $n = 5$ , and with Tukey's post test.

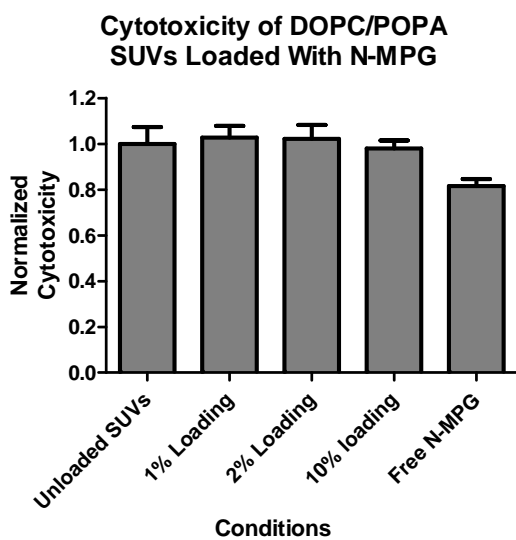


Figure 25: Cytotoxicity of DOPC/POPA SUVs Loaded with N-MPG. No significant cytotoxic effects were seen as tested by ANOVA,  $p < 0.05$ ,  $n = 5$ , and with Tukey's post test.

### 3.4 SUV Antioxidant Capacity

#### 3.4.1 SUV Hydroperoxidation

Determining SUV hydroperoxidation was necessary in order to determine if lipid degradation was producing peroxides that would take away from antioxidant capacity. The results of Figure 23 indicate that there is less than 0.2 nmoles of lipid hydroperoxides in both SUV compositions. This indicates that oxidative degradation of the lipids happens slowly enough that there is negligible peroxidation of the SUVs before they are subjected to hydrogen peroxide based antioxidant capacity evaluation.

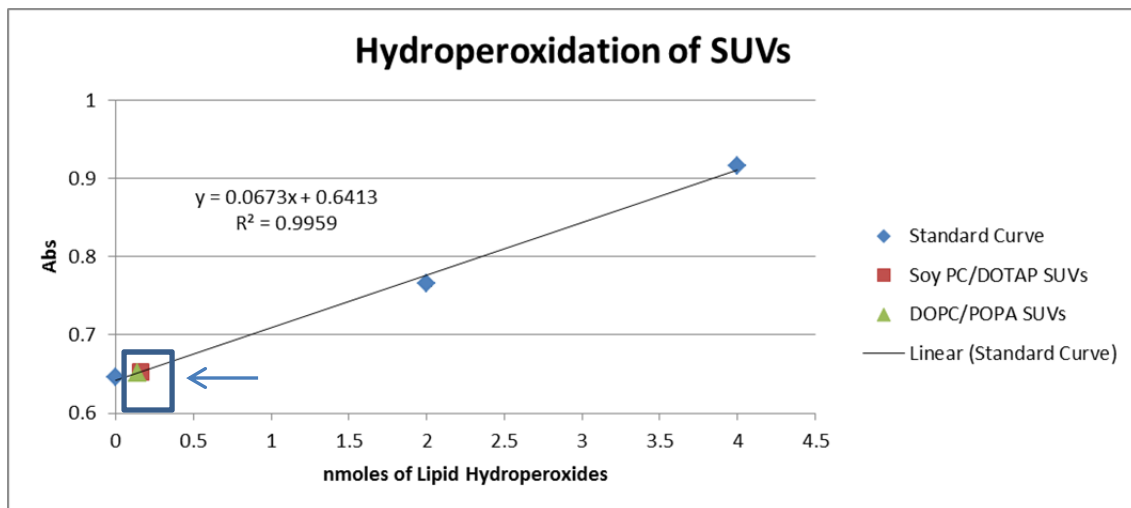


Fig 26: 48 Hour Lipid Hydroperoxidation

#### 3.4.2 SUV Pre-Incubation Time for Antioxidant Capacity

Based on the visually estimated level of fluorescence shown by curcumin in the HDFs, it was determined that SUV delivery occurs after 1 minute of incubation time and that there was no noticeable reduction of curcumin in the cells through 40 minutes of

incubation. The Soy-PC/DOTAP images were taken using Metamorph software and the DOPC/POPA images were taken using NIS Elements software. Because curcumin photo-bleaches quickly and image capturing was taken by hand instead of automated, quantification of the fluorescence would not be accurate and so quantification of the fluorescence seen in the images would not be accurate. Previous data from our group showed that peak curcumin levels occurred at 15 minutes and showed no decrease until 30 minute incubation. Based on fluorescent estimates of the curcumin levels and previous SUV data by our group, a pre-incubation time of 20 minutes was used for antioxidant capacity assays.

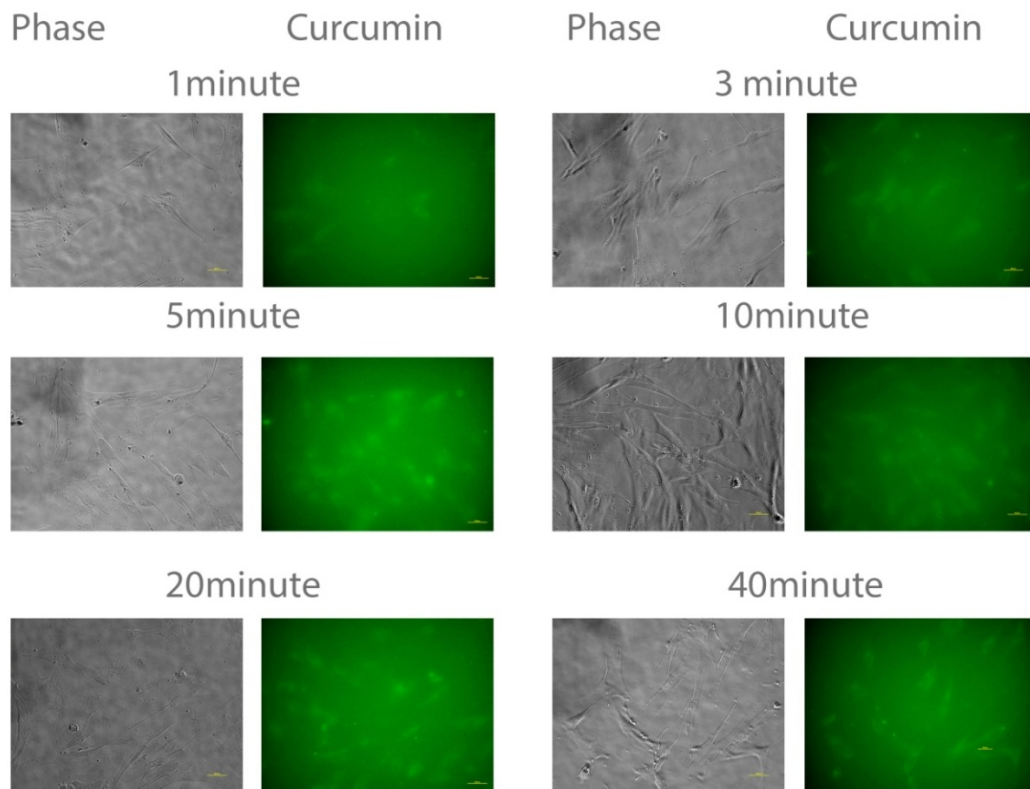


Figure 27: Pre-Incubation Images for Soy-PC/DOTAP SUVs at 10x magnification.

Images show that curcumin is present in the cells at all timepoints

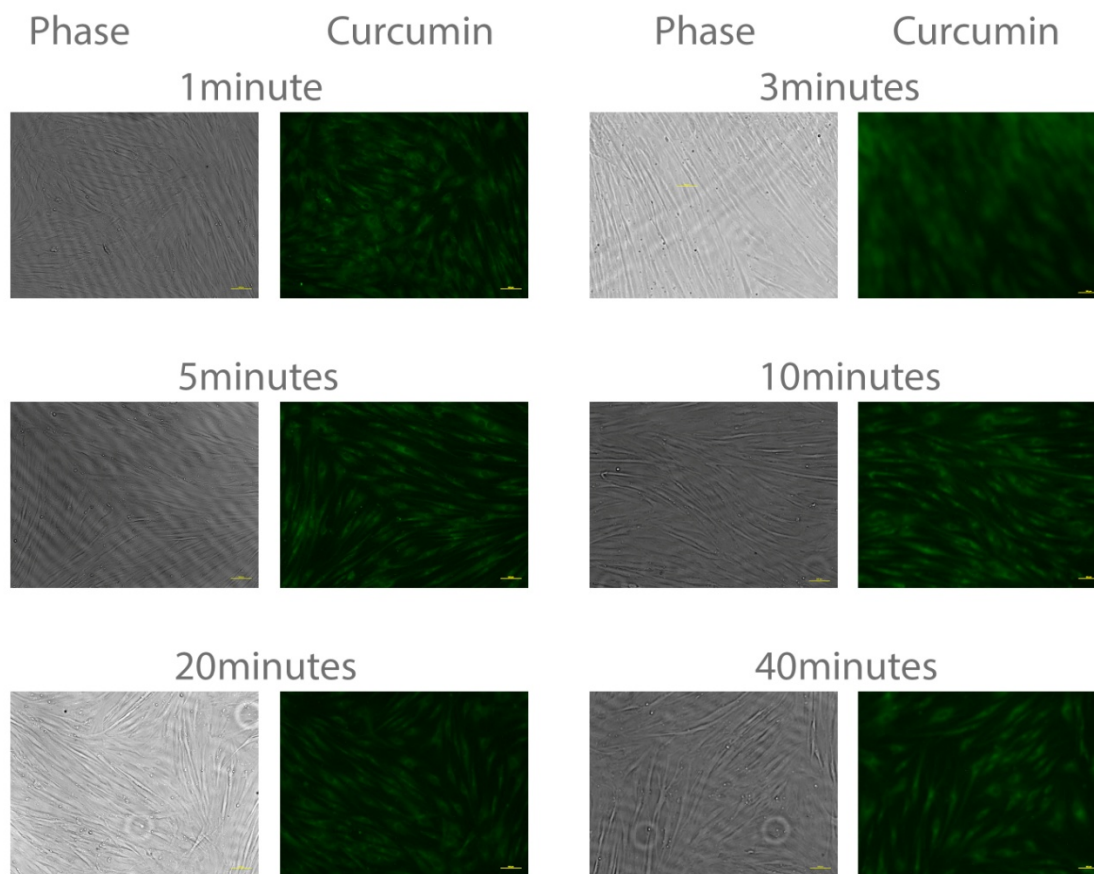


Figure 28: Pre-incubation images for DOPC/POPA SUVs at 10x magnification . Images show that curcumin is in the cells at all timepoints.

### 3.4.3 Amplex Red Hydrogen Peroxide Assay

Antioxidant capacity is used to demonstrate the efficacy of the antioxidants against ROS as simulated by hydrogen peroxide. Statistical analysis of curcumin loaded SUVs (Figures 29 and 30) showed that all loading conditions except for DOPC/POPA SUVs loaded with 1% curcumin created a significant peroxide reduction from unloaded SUVs. Statistical analysis also showed that the beyond 1% loading Soy-PC/DOTAP curcumin loading conditions exhibited a significant peroxide reduction when compared to

DOPC/POPA. Finally statistics showed that free curcumin had a significant peroxide reduction compared to DOPC/POPA SUVs loaded with 10% curcumin but not compared to Soy-PC/DOTAP SUVs loaded with 10% curcumin. After the addition of the hydrogen peroxide and Amplex Red dye, 10% curcumin treatments had  $16.3\mu\text{M}$  curcumin and  $25\mu\text{M}$  hydrogen peroxide. From this, the normalized peroxide reduction was used to calculate that 1.5, 1.6, and 1.9 moles of free curcumin, Soy-PC/DOTAP loaded with 10% curcumin, and DOPC/POPA loaded with 10% curcumin respectively were used to eliminate 1 mole hydrogen peroxide. This implies that there is no loss in antioxidant function due to fabrication for Soy-PC/DOTAP SUVs.

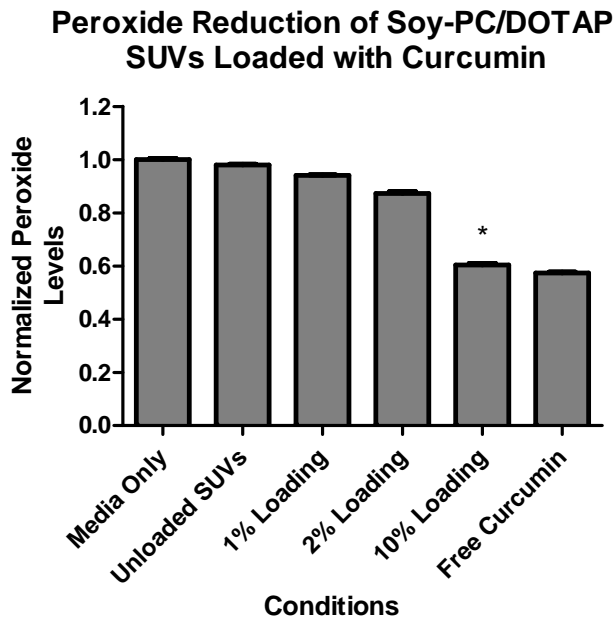


Figure 29: Peroxide Reduction of Soy-PC/DOTAP SUVs Loaded with Curcumin.

\*=Significant difference from all other groups except for free curcumin as tested by ANOVA,  $n=4$ ,  $p<0.05$ , with Tukey's post test.



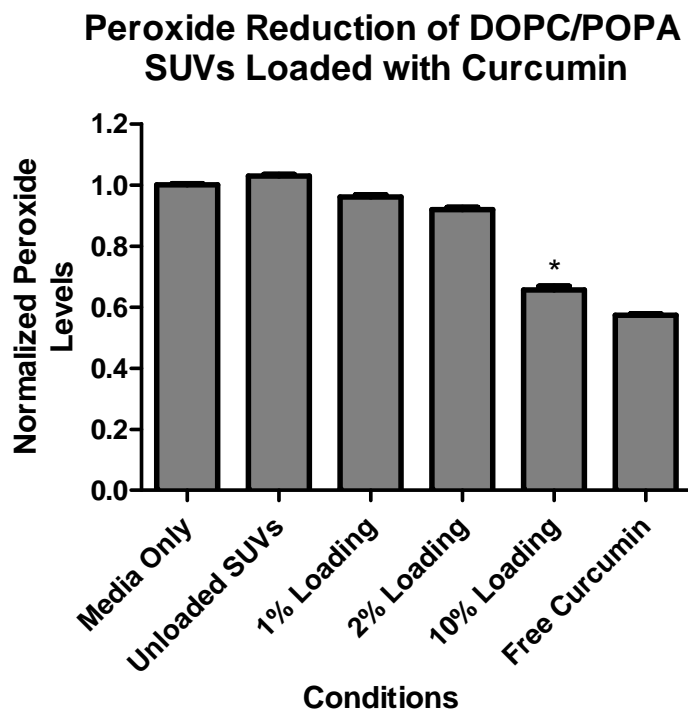


Figure 30: Peroxide Reduction of DOPC/POPA SUVs Loaded with Curcumin.

\*=Significant difference from all other groups as tested by ANOVA,  $n=4$ ,  $p<0.05$ , with Tukey's post test.

Statistical analysis of NAC loaded SUVs (Figures 31 and 32) showed that there was no significant peroxidation decrease from unloaded conditions for DOPC/POPA until 10% NAC loading was reached while Soy-PC/DOTAP loading conditions reached significance at 2% NAC loading concentrations. Statistical analysis of Figures 31 and 32 also showed that free NAC showed a significant decrease in peroxidation from DOPC/POPA SUVs loaded with 10% NAC but not from Soy-PC/DOTAP SUVs loaded with 10% NAC. After the addition of the hydrogen peroxide and Amplex Red dye, 10% NAC treatments had  $76.5\mu\text{M}$  NAC and  $25\mu\text{M}$  hydrogen peroxide. From this, the normalized peroxide reduction was used to calculate that 5.5, 5.9, and 6.4 moles of free

NAC, Soy-PC/DOTAP SUVs loaded with 10% NAC, and DOPC/POPA SUVs loaded with 10% NAC respectively were used to eliminate 1 mole hydrogen peroxide. This implies that there was significant loss in antioxidant function for NAC loaded DOPC/POPA SUVs during production but not for the Soy-PC/DOTAP counterparts. The moles of NAC required to neutralize 1 mole of hydrogen peroxide is much higher than the moles of curcumin required for the same effect which could potentially be attributed to spontaneous formation of disulfide bonds between NAC molecules.

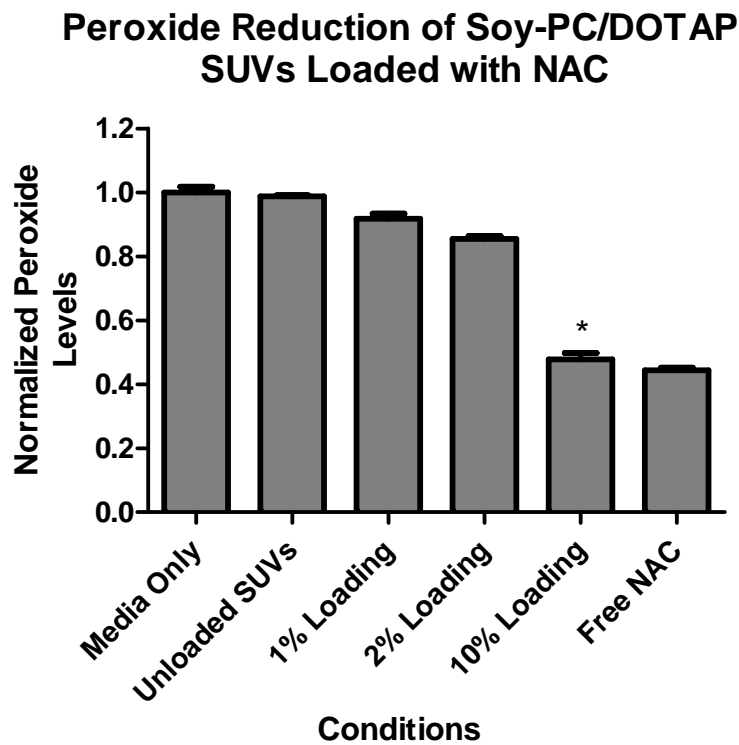


Figure 31: Peroxide Reduction of Soy-PC/DOTAP SUVs Loaded with NAC.

\*=Significant difference from all other groups except for free NAC as tested by ANOVA,  $n=4$ ,  $p<0.05$ , with Tukey's post test.

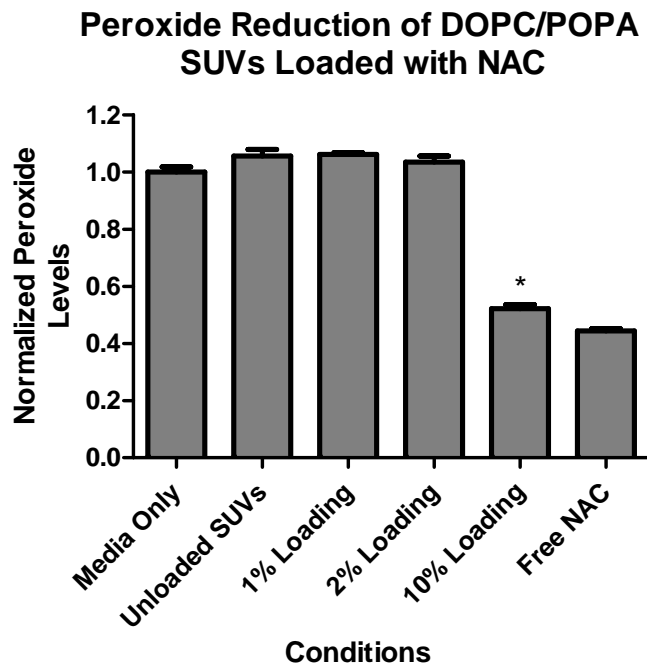


Figure 32: Peroxide Reduction of DOPC/POPA SUVs Loaded with NAC. \*=Significant difference from all other groups as tested by ANOVA,  $n=4$ ,  $p<0.05$ , with Tukey's post test.

Statistical analysis of N-MPG loaded SUVs (Figures 33 and 34) showed that there was no significant peroxidation decrease from unloaded conditions for DOPC/POPA until 10% N-MPG loading was reached while Soy-PC/DOTAP loading conditions reached significance at 2% N-MPG loading concentrations. Statistical analysis of Figures 33 and 34 also showed that there was a statistical difference in peroxide reduction between free N-MPG, DOPC/POPA SUVs loaded with 10% N-MPG, and Soy-PC/DOTAP SUVs loaded with 10% N-MPG. Soy-PC/DOTAP SUVs loaded with 10% N-MPG therefore, had significantly less peroxide reduction from free N-MPG but significantly more reduction than DOPC/POPA SUVs loaded with 10% N-MPG. This implies that there is a significant decrease in antioxidant function for N-MPG loaded

SUVs for both compositions. After the addition of the hydrogen peroxide and Amplex Red dye, 10% N-MPG treatments had 76.5 $\mu$ M N-MPG and 25 $\mu$ M hydrogen peroxide. From this, the normalized peroxide reduction was used to calculate that 4.7, 5.6, and 7.9 moles of free N-MPG, Soy-PC/DOTAP SUVs loaded with 10% N-MPG, and DOPC/POPA SUVs loaded with 10% N-MPG respectively were used to eliminate 1 mole hydrogen peroxide. The moles of N-MPG required to neutralize 1 mole of hydrogen peroxide is much higher than the moles of curcumin required for the same effect which could be attributed to the formation of disulfide bonds between N-MPG molecules.

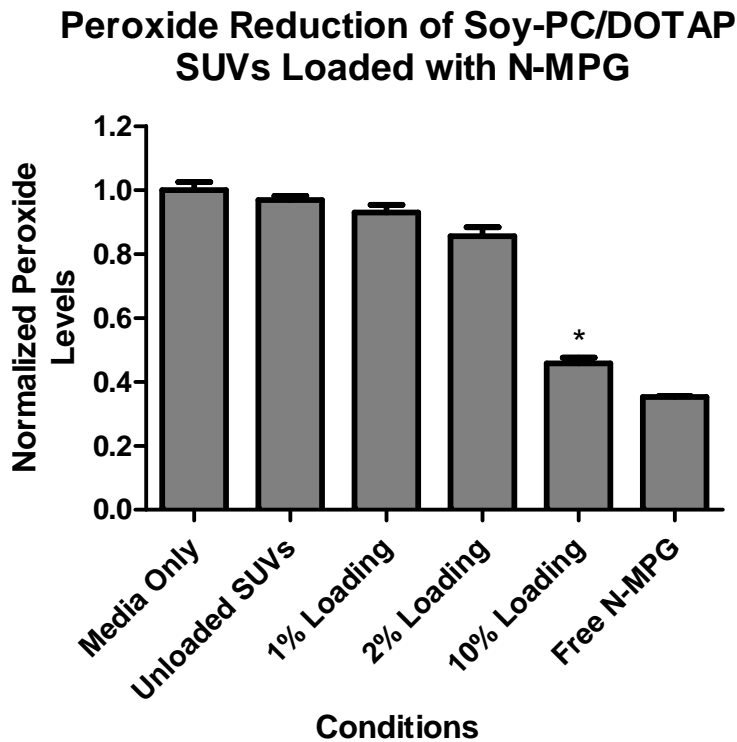


Figure 33: Peroxide Reduction of Soy-PC/DOTAP SUVs Loaded with N-MPG.

\*=Significant difference from all other groups as tested by ANOVA, n=4, p<0.05, with Tukey's post test.

### Peroxide Reduction of DOPC/POPA SUVs Loaded with N-MPG

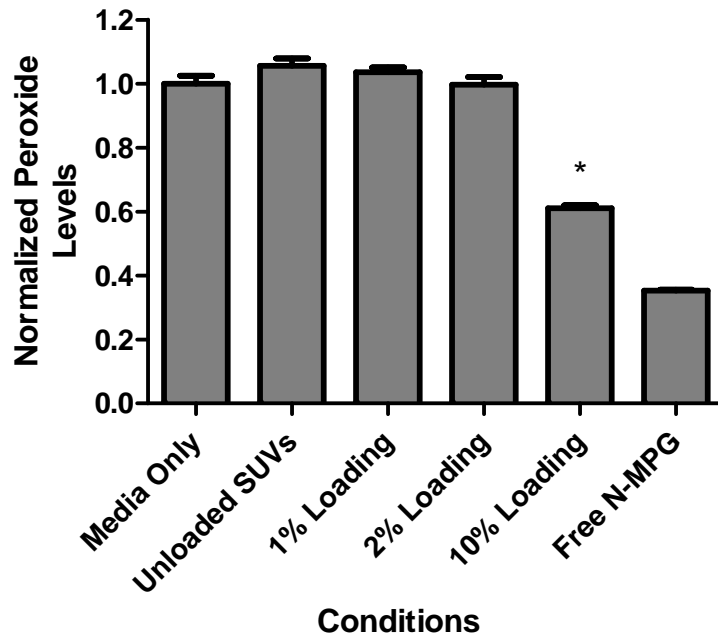


Figure 34: Peroxide Reduction of DOPC/POPA SUVs Loaded with N-MPG.

\*=Significant difference from all other groups as tested by ANOVA, n=4, p<0.05, with Tukey's post test.

#### IV. CONCLUSIONS, DISCUSSION, AND FUTURE WORK

The low theoretical encapsulation efficiency could become a major obstacle in the use of SUVs for the delivery of hydrophilic materials. This low encapsulation efficiency could be offset by increasing the concentration of the lipids in solution before sonication although that would change the time for the limiting hydrodynamic radius to be reached. This could also be offset by increasing the concentration of the material to be entrapped with cytotoxicity being the limiting factor. Both of these parameter changes should be explored and needed based on required therapeutic concentrations of hydrophilic material. A size exclusion column to separate unencapsulated material followed by the use of HPLC could be used to obtain a loading efficiency for hydrophilic materials in a SUV.

While not statistically significant, it should be noted that DOPC/POPA SUVs had less cytotoxicity compared to Soy-PC/DOTAP SUVs which may become important if Soy-PC/DOTAP SUVs demonstrate significant toxicity with other cell lines. In order to reduce overall toxicity for future cell studies, SUV production at higher lipid concentrations should be investigated in order to mitigate the negative effects of diluting the media when adding SUV treatments.

DOPC/POPA SUVs for all 10% loading conditions consistently showed significantly lower antioxidant function compared to respective loading conditions of Soy-PC/DOTAP implies that the antioxidant function is better preserved in Soy-PC/DOTAP SUVs. To supplement data from the Amplex Red assay, a delivery profile would be the next ideal step. Degradation based release profile techniques do not apply to

fusogenic SUVs since their mechanism of delivery is fusion rather than degradation making the tracking of released antioxidants require the presence of cells. Nile Red is a lipophilic fluorescent dye that may be able to track the SUV fusion and should be investigated. An initial potential obstacle to fluorescent tracking is that cells with excess lipid in their membranes will bleb off small portions of the membrane which may limit the extent to which delivery can be tracked[20].

In summary the research indicated that antioxidant loaded SUVs can be consistently produced through sonication for both lipid compositions and all antioxidant loading conditions using DLS measurements. All SUV treatments produced were shown to not have significant cytotoxic effects on HDFs. Of those treatments, Soy-PC/DOTAP SUVs loaded with curcumin and loaded with NAC showed no significant loss in antioxidant function after the fabrication process. For future evaluation in cell environments exposed to radiation, it is recommended that both the Soy-PC/DOTAP SUVs loaded with curcumin be explored due to the high encapsulation efficiencies and the maintained antioxidant capacity when compared to the free antioxidants.

## V. REFERENCES

1. Goodhead, D.T., *Initial events in the cellular effects of ionizing radiations: clustered damage in DNA*. Int J Radiat Biol, 1994. **65**(1): p. 7-17.
2. Singh, A.K., *Impact of galactic cosmic rays on Earth's atmosphere and human health*. Atmospheric Environment, 2011. **45**(23): p. 3606-3818.
3. Hei, T.K., et al., *Mechanism of radiation-induced bystander effects: a unifying model*. J Pharm Pharmacol, 2008. **60**(8): p. 943-50.
4. Lomax, M.E., L.K. Folkles, and P. O'Neill, *Biological consequences of radiation-induced DNA damage: relevance to radiotherapy*. Clin Oncol (R Coll Radiol), 2013. **25**(10): p. 578-85.
5. *Reactive Oxygen Species*. 2014; Available from: www.nature.com.
6. Durante, M. and F.A. Cucinotta, *Heavy ion carcinogenesis and human space exploration*. Nat Rev Cancer, 2008. **8**(6): p. 465-72.
7. Raviraj, J., et al., *Radiosensitizers, radioprotectors, and radiation mitigators*. Indian J Dent Res, 2014. **25**(1): p. 83-90.
8. Shao, Z.M., et al., *Curcumin exerts multiple suppressive effects on human breast carcinoma cells*. Int J Cancer, 2002. **98**(2): p. 234-40.
9. Sharma, R.A., A.J. Gescher, and W.P. Steward, *Curcumin: the story so far*. Eur J Cancer, 2005. **41**(13): p. 1955-68.
10. Anand, P., et al., *Bioavailability of curcumin: problems and promises*. Mol Pharm, 2007. **4**(6): p. 807-18.
11. Shen, L. and H.F. Ji, *The pharmacology of curcumin: is it the degradation products?* Trends Mol Med, 2012. **18**(3): p. 138-44.
12. Priyadarsini, K.I., *Free radical reactions of curcumin in membrane models*. Free Radic Biol Med, 1997. **23**(6): p. 838-43.
13. Adhikari, S., K. Indira Priyadarsini, and T. Mukherjee, *Physico-chemical studies on the evaluation of the antioxidant activity of herbal extracts and active principles of some Indian medicinal plants*. J Clin Biochem Nutr, 2007. **40**(3): p. 174-83.
14. Wang, Y.J., et al., *Stability of curcumin in buffer solutions and characterization of its degradation products*. J Pharm Biomed Anal, 1997. **15**(12): p. 1867-76.
15. Heard, K.J., *Acetylcysteine for acetaminophen poisoning*. N Engl J Med, 2008. **359**(3): p. 285-92.
16. Navath, R.S., et al., *Dendrimer-drug conjugates for tailored intracellular drug release based on glutathione levels*. Bioconjug Chem, 2008. **19**(12): p. 2446-55.
17. Mari, M., et al., *Mitochondrial glutathione, a key survival antioxidant*. Antioxid Redox Signal, 2009. **11**(11): p. 2685-700.
18. Pendyala, L. and P.J. Creaven, *Pharmacokinetic and pharmacodynamic studies of N-acetylcysteine, a potential chemopreventive agent during a phase I trial*. Cancer Epidemiol Biomarkers Prev, 1995. **4**(3): p. 245-51.
19. Zeida, A., et al., *Molecular basis of the mechanism of thiol oxidation by hydrogen peroxide in aqueous solution: challenging the SN2 paradigm*. Chem Res Toxicol, 2012. **25**(3): p. 741-6.
20. Coe, F.L., J.H. Parks, and J.R. Asplin, *The pathogenesis and treatment of kidney stones*. N Engl J Med, 1992. **327**(16): p. 1141-52.



21. Herculín, B., et al., *The pharmacokinetics of tiopronin and its principal metabolite (2-mercaptopropionic acid) after oral administration to healthy volunteers*. Eur J Clin Pharmacol, 1992. **43**(1): p. 93-5.
22. Xu, X., M.A. Khan, and D.J. Burgess, *Predicting hydrophilic drug encapsulation inside unilamellar liposomes*. Int J Pharm, 2012. **423**(2): p. 410-8.
23. Kunisawa, J., et al., *Fusogenic liposome delivers encapsulated nanoparticles for cytosolic controlled gene release*. J Control Release, 2005. **105**(3): p. 344-53.
24. Kunwar, A., et al., *Transport of liposomal and albumin loaded curcumin to living cells: an absorption and fluorescence spectroscopic study*. Biochim Biophys Acta, 2006. **1760**(10): p. 1513-20.
25. Hoblitzell, P., *CHARACTERIZATION, DELIVERY, AND EFFECTS OF CURCUMIN LOADED LIPOSOME VESICLES*, in *Bioengineering*. 2010, University of Louisville: Louisville, KY
26. Ehringer, W.D., *Preserved Fusogenic Vesicles*. 2006: United States.
27. Lipids, A.P. *Products*. 2014; Available from: [https://www.avantilipids.com/index.php?option=com\\_content&view=article&id=3&Itemid=7](https://www.avantilipids.com/index.php?option=com_content&view=article&id=3&Itemid=7).
28. Kraft, J.C., et al., *Emerging research and clinical development trends of liposome and lipid nanoparticle drug delivery systems*. J Pharm Sci, 2014. **103**(1): p. 29-52.
29. Gast, K. and C. Fiedler, *Dynamic and static light scattering of intrinsically disordered proteins*. Methods Mol Biol, 2012. **896**: p. 137-61.

## BRIAN GETTLER

631 Bellamy Circle Apt# 307,  
Louisville, KY 40208

---

---

Phone:859.312.8118

Email:bcgett01@gmail.com

Bioengineering graduate searching for full time employment with 2+ years of laboratory experience in biological wet laboratories. Experience in cell culture methods for yeast and human dermal fibroblasts. Additional experience in electrospon cellular scaffolds and lipid based nanoparticles.

### EXPERIENCE

---

#### University of Louisville & Energy Delivery Solutions

##### Research Engineer

August 2013-Present

Masters of Engineering thesis to evaluate the efficacy of antioxidants used in a radio-protective role.

- Optimized and manufactured lipid vesicle delivery system for antioxidants
- Tested efficacy of delivery system and antioxidants *in vitro* with fibroblasts

#### Cardiovascular Innovation Institute, Louisville, KY

##### Research Engineer

January 2013-

July 2013

Worked independently to manufacture and evaluate cellular scaffolds for potential use in a clinical pilot trial

- Manufactured bio-absorbable cell scaffolds for fistula plugs via electrospinning
- Performed *in vitro* evaluations on scaffolds for cell seeding and infiltration
- Helped prepare 1<sup>st</sup> human clinical trial

#### Allylix, Lexington, KY

##### Research Engineer/Research Associate

May 2012-

August 2012

Worked as a technician with a primary project of assay troubleshooting and secondary tasks of recombinant yeast mutant screenings. Additional tasks of laboratory cleaning and maintenance.

- Troubleshot an assay for gas chromatography based micro-culture screening
- Performed yeast/E. Coli transformations (plasmid and recombinant)
- Performed micro-culture mutant screening and shake flask mutant screening

**Alltech**, Lexington, KY

**Laboratory Technician**

August 2011-

December 2011

Worked independently to manufacture and evaluate a bioremediation product with long term goal of EPA submission.

- Manufactured bioremediation product for testing
- Data analysis tests performed on product for EPA submission purposes
- Data was focused on product growth rates and target material degradation rates
- Displayed results in an open presentation

---

**EDUCATION**

---

**Bachelors of Science**, Bioengineering, University of Louisville, Louisville, KY, 3.13 GPA, July 2013

**Masters of Engineering**, Bioengineering, University of Louisville, Louisville, KY, 3.51 GPA,  
Expected December 2014

---

**TECHNICAL SKILLS**

---

**Lab Skills**: Cell culture (flask and microscale), sterile technique, fluorescent staining & imaging, H&E staining, most probable number test, pH, agar plating, selection marker use (i.e. uracil, leucine), DNA/protein gels & extractions, PCR, optical density measurements

**Lab Equipment Used**: probe sonicator, SEM, electrospinner, steam autoclave, pH meter, centrifuge, fluid bed dryer, Rotovap distillation setup, gas chromatograph, 96 well plates, various pipets.

Some experience in: Minitab, Labview, Matlab